2003-06

# An evaluation of electric motors for ship propulsion

Bassham, Bobby A.

Monterey, California. Naval Postgraduate School

# NAVAL POSTGRADUATE SCHOOL
## Monterey, California


# THESIS

**AN EVALUATION OF ELECTRIC MOTORS FOR SHIP PROPULSION**

by

Bobby A. Bassham

June 2003

| | |
|---|---|
| Thesis Advisor: | Robert Ashton |
| Second Reader: | Todd Weatherford |

**Approved for public release; distribution is unlimited**

THIS PAGE INTENTIONALLY LEFT BLANK

# REPORT DOCUMENTATION PAGE

*Form Approved OMB No. 0704-0188*



| 1. AGENCY USE ONLY *(Leave blank)* | 2. REPORT DATE | 3. REPORT TYPE AND DATES COVERED |
|---|---|---|
| | June 2003 | Master's Thesis |

**4. TITLE AND SUBTITLE** An Evaluation of electric motors for ship propulsion

**5. FUNDING NUMBERS**

**6. AUTHOR (S) Bobby A. Bassham**

**7. PERFORMING ORGANIZATION NAME(S) AND ADDRESS(ES)**
Naval Postgraduate School
Monterey, CA 93943-5000

**8. PERFORMING ORGANIZATION REPORT NUMBER**

**9. SPONSORING / MONITORING AGENCY NAME(S) AND ADDRESS(ES)**

**10. SPONSORING/MONITORING AGENCY REPORT NUMBER**

**11. SUPPLEMENTARY NOTES** The views expressed in this thesis are those of the author and do not reflect the official policy or position of the U.S. Department of Defense or the U.S. Government.

**12a. DISTRIBUTION / AVAILABILITY STATEMENT**
Approved for public release; distribution is unlimited.

**12b. DISTRIBUTION CODE**

**13. ABSTRACT** ***(maximum 200 words)***

An evaluation was conducted of the various propulsion motors being considered for electric ship propulsion. The benefit of such an evaluation is that all of the propulsion options being considered by the U.S. Navy have been described in one document. The AC induction motor, AC synchronous motor, High Temperature Superconducting (HTS) motor and Superconducting DC Homopolar Motor (SDCHM) are examined. The properties, advantages, and disadvantages of each motor are discussed and compared. The power converters used to control large propulsion motors are also discussed. The Navy's IPS program is discussed and the results of concept testing are presented. Podded propulsion is introduced and the benefits are discussed. The final chapter presents the simulation results of a volts/Hertz controlled 30 MW induction motor. The evaluation revealed that the permanent magnet motor is the best propulsion motor when considering mature technology, power density, and acoustic performance. HTS motors offer significant volume reductions and improved acoustic performance as compared to conventional motors. This includes both AC and DC HTS motors. The main obstacle for the SDCHM remains the unavailability of high current capacity brushes.

| 14. SUBJECT TERMS: Electric Propulsion, Electric Ship, Integrated Power System, Induction Motor, Permanent Magnet Motor, HTS Synchronous Motor, DC Homopolar Motor, Podded Propulsion. | 15. NUMBER OF PAGES 117 |
|---|---|
| | 16. PRICE CODE |

| 17. SECURITY CLASSIFICATION OF REPORT | 18. SECURITY CLASSIFICATION OF THIS PAGE | 19. SECURITY CLASSIFICATION OF ABSTRACT | 20. LIMITATION OF ABSTRACT |
|---|---|---|---|
| Unclassified | Unclassified | Unclassified | UL |

**NSN 7540-01-280-5500** **Standard Form 298 (Rev. 2-89)**
**Prescribed by ANSI Std. 239-18**

THIS PAGE INTENTIONALLY LEFT BLANK

**Approved for public release; distribution is unlimited.**

**AN EVALUATION OF ELECTRIC MOTORS FOR SHIP PROPULSION**

Bobby A. Bassham
Ensign, United States Navy
BEE, Auburn University, 2002

Submitted in partial fulfillment of the
requirements for the degree of

**MASTER OF SCIENCE IN ELECTRICAL ENGINEERING**

from the

**NAVAL POSTGRADUATE SCHOOL**
**June 2003**

Author: Bobby A. Bassham

Approved by: Professor Robert Ashton
Thesis Advisor

Professor Todd Weatherford
Second Reader

John P. Powers
Chairman, Department of Electrical and Computer Engineering

THIS PAGE INTENTIONALLY LEFT BLANK

# ABSTRACT

An evaluation was conducted of the various propulsion motors being considered for electric ship propulsion. The benefit of such an evaluation is that all of the propulsion options being considered by the U.S. Navy have been described in one document. The AC induction motor, AC synchronous motor, High Temperature Superconducting (HTS) motor and Superconducting DC Homopolar Motor (SDCHM) are examined. The properties, advantages, and disadvantages of each motor are discussed and compared. The power converters used to control large propulsion motors are also discussed. The Navy's IPS program is discussed and the results of concept testing are presented. Podded propulsion is introduced and the benefits are discussed. The final chapter presents the simulation results of a volts/Hertz controlled 30 MW induction motor. The evaluation revealed that the permanent magnet motor is the best propulsion motor when considering mature technology, power density, and acoustic performance. HTS motors offer significant volume reductions and improved acoustic performance as compared to conventional motors. This includes both AC and DC HTS motors. The main obstacle for the SDCHM remains the unavailability of high current capacity brushes.

THIS PAGE INTENTIONALLY LEFT BLANK

## TABLE OF CONTENTS

# LIST OF FIGURES

## LIST OF TABLES

THIS PAGE INTENTIONALLY LEFT BLANK

## ACKNOWLEDGEMENTS

I would like to thank the United States Navy for giving me the opportunity to study at the Naval Postgraduate School. I would also like to thank the many professors at NPS for unselfishly sharing their knowledge with me. Finally, I am most grateful to my wife and son for being so understanding while I pursued my academic career.

THIS PAGE INTENTIONALLY LEFT BLANK

## EXECUTIVE SUMMARY

The U.S. Navy is currently developing an all-electric ship that will employ an Integrated Power System (IPS) and Integrated Electric Drive (IED). The IPS concept was proven by the Navy's land-based IPS test site in Philadelphia, PA. Future ships will employ electric prime movers instead of using the mechanical gas turbine drives found on nearly all of the Navy's surface combatants. The benefits achievable through the use of an IPS and IED include increased efficiency, increased reliability and survivability, reduced fuel costs, and reduced manpower requirements. These benefits are possible because an IPS and IED require fewer prime movers and auxiliary equipment than conventional propulsion systems.

Several electric motors are being researched and developed for possible use in surface ships. The motor types include induction, permanent magnet, high temperature superconducting AC, and high temperature superconducting DC motors. Each motor is discussed in this study.

The AC induction motor offers a robust design and high power density. The induction motor was used by the Navy to demonstrate the feasibility of employing an IPS on a surface ship. The U.K. has also selected the induction motor to be the prime mover in their Type-45 destroyer. Alstom Corporation is leading the industry in induction motor development with their Advanced Induction Motor (AIM).

Permanent magnet motors are more power dense than a comparatively sized induction motor. The permanent magnet motor has been chosen to provide propulsion power in the Navy's DD(x) destroyer. They are also acoustically quieter. Three types of permanent magnet motor are discussed in this study. They include the axial flux, the radial flux, and the transverse flux permanent magnet motors. Each motor has its unique advantages.

High Temperature Superconducting AC (HTSAC) synchronous motors offer significant volume and weight reductions as compared to conventional motors. This is made possible because HTS wire has a much higher current density than conventional copper wire. Significant size reductions can be realized by using HTS wire in rotor construction.

The drawback to this technology is the requirement of keeping the HTS windings at a very low operating temperature. American Superconductor Corporation (AMSC) is currently leading the industry in HTS motor development. AMSC is currently under contract with the Office of Naval Research (ONR) to develop an HTS AC motor for ship propulsion.

The Superconducting DC Homopolar Motor (SDCHM) also uses HTS wire for rotor construction. The Navy first demonstrated the SDCHM in the early 1980's in the NSWC test craft *Jupiter II*. That motor used Low Temperature Superconducting (LTS) winding. LTS windings are susceptible to quenching, so they are not being pursued for use in current homopolar designs. General Atomics Corporation is developing the homopolar motor in the U.S. for possible propulsion applications.

Podded propulsion can potentially increase propulsion efficiency by as much as 15%. Pods are widespread in the commercial shipping industry and in cruise liners. The Navy is researching them for possible use in surface ships. Pods reduce the amount of installed equipment and totally eliminate the need for long shaft lines.

Several different types of converters are used to provide ideal operating power for the motors discussed in this study. Some of them include cycloconverters, synchroconverters, Pulse Width Modulated (PWM) converters, and Pulse Frequency Modulated (PFM) converters. PWM converters can be either voltage source or current source inverters. Power semiconductor device technology is driving power converter technology. Power converters are limited by the voltage and switching characteristics of the semiconductor devices.

The final chapter includes 30-MW induction motor simulation that uses volts/Hertz control. Upon comparison with the simulation of a smaller motor, the simulation results revealed that the volts/Hertz control method is not sufficient for very large motors. The larger motor did not follow its commanded speed during load fluctuations and there were also excessive torque pulsations that are undesirable.

# I. INTRODUCTION

## A. INTRODUCTION TO IPS AND ELECTRIC PROPULSION

Mechanical propulsion drives have dominated naval surface ship propulsion for the past half-century. The Navy's newest warships will rely on electric propulsion and will incorporate an Integrated Power System (IPS). The basic principle of an IPS is that the same generators can be used to provide power for propulsion and ship services. The ability to use the same prime mover to provide all of the ship's power needs will reduce the number of installed prime movers and their associated equipment. This will unlock propulsion power for other uses and help reduce fuel, maintenance, and manning costs throughout a ship's lifecycle. The DD(x) destroyer will be the first U.S. Navy ship to employ an IPS and Integrated Electric Drive (IED).

### 1. Background on the DD(x)

#### *a. DD-21 Zumwalt Class*

At the end of the Cold War, the U.S. Navy identified the need for an advanced warship capable of countering the threats of the Post-Cold War era. Specifically, the Navy wanted a ship with the capability of operating in and dominating littoral battle areas. The new ship was initially named the DD-21 land attack destroyer. In July 2000, President Clinton named the ship the DD-21 Zumwalt class destroyer, after the late ADM Elmo R. Zumwalt, Jr.

#### *b. DD(x)*

In November, 2001 the Navy announced that it would rename the DD-21 and call it the DD(x) to accurately reflect the program's purpose which is to produce a family of advanced surface combatants and not just a single ship class. Other ships under DD(x) could include the advanced cruiser CG(x) and the Littoral Combat Ship (LCS). These ships will employ advanced weapon systems, multifunction radars, IPS, and IED.

## B. HISTORY OF ELECTRIC PROPULSION AND IPS

### 1. Historical Use of Electric Drives on Surface Combatants

The use of electric propulsion is not a new concept for the U.S. Navy. As far back as 1913, the Navy Collier Jupiter – which was converted to America's first aircraft carrier – U.S.S Langley, used electric propulsion [1]. Langley's propulsion system used steam-powered turbine generators and Alternating Current (AC) propulsion motors [1]. The success of the propulsion system prompted the use of electric drive in U.S.S New Mexico and five successor battleships [1]. The Navy's second and third aircraft carriers, U.S.S Lexington and U.S.S Saratoga also used a turbo-electric drive [1].

#### *a. Geared Turbines Replaced Electric Drives*

During the 1930's, electric drives were phased-out in favor of geared-turbine drives [1]. This was made possible by the improvements being made in reduction gear technology [1]. The geared turbine drive was both smaller and lighter than the electric drive and was able to meet the Navy's requirements for ever-higher speed [1]. Mechanical or geared propulsion has been used in surface combatants ever since.

#### *b. The Return to Electric Propulsion*

Technological advances have enabled the return of electric drives in surface combatants. Beginning approximately fifteen years ago, advances in high-powered AC motors led to their growing use in cruise ships, cargo carriers, and cable layers [1]. Even prior to this, the Navy was researching the use of superconducting and homopolar motors to increase the power density of shipboard electric machines [1]. In the early 1980's, the Navy demonstrated a 3,000 HP superconducting homopolar drive on the *Jupiter II* test craft [1]. Because of further improvements in superconducting material technology, the Navy is once again researching the superconducting DC homopolar motor for ship propulsion. The Navy is also investigating high temperature superconducting AC synchronous motors, permanent magnet synchronous motors, and induction motors for ship propulsion.

## C. PROPULSION OPTIONS FOR THE ELECTRIC SHIP

One of the most important considerations in a new ship design is the method of propulsion to be used. By using electric motors for propulsion, shipbuilders will no longer be constrained by the placement of an in-line reduction gear and shaft placement. With proper motor selection, electric propulsion can eliminate the need for a reduction gear and significantly reduce the length of the shaft (or eliminate it altogether).

### 1. Possible Configurations

The Navy has been investigating two methods of electric propulsion for possible use in a future ship design. The first uses a prime mover and shaft configuration, similar to the mechanical drives found in nearly all surface ships. This method is considered in-hull propulsion. The second method uses direct-drive podded propulsors similar to those found in commercial shipping and in cruise liners. Although the Navy has decided not to use podded propulsion in its newest ship, the method will be discussed in this study because of its potential use in later ship designs.

#### *a. In-Hull Propulsion*

In this configuration, the prime mover is located inside the hull of the ship. Rotational torque is transferred to the propeller by using a shaft that extends aft from the prime mover and penetrates the hull of the ship. The propeller is connected to the end of the shaft and converts rotational torque into forward and reverse thrust. This method of propulsion requires additional equipment such as shaft bearings at bulkhead penetrations, shaft seals at hull penetrations, and a rudder to provide steering control for the vessel. With the exception of an electric prime mover, this method is currently employed in all surface combatants. Although this method still requires the use of a shaft, significant reductions in shaft length are possible due to increased flexibility in locating the prime mover within the ship.

#### *b. Podded Propulsion*

The second propulsion method involves the use of Podded Propulsors (Pods). Pods are widespread in the cruise liner industry and in commercial shipping. Pods can be directly driven or indirectly driven. In a direct driven pod, the prime mover

is located outside of the ship's hull inside an enclosure or pod. This allows the propeller to be mounted directly to the prime mover, eliminating the need for an in-hull shaft. Indirectly driven propulsors, also known as azimuthing thrusters, usually have their prime mover located inside the ship. In this configuration, a gearing mechanism connects the prime mover to the propulsor. The Navy is mainly interested in direct driven propulsors due to the increased noise level associated with the gearing in the indirect method [2]. Direct drive pods eliminate the need for a shaft and overcome the problems associated with hull penetrations. Since the propulsion pod is mounted to the ship's hull, steering control can be obtained simply by allowing the pod to rotate through 360°. This capability eliminates the need for a rudder. Changing the prime mover's direction of rotation provides forward and reverse thrust.

### 2. Competing Electric Motor Technologies

#### *a. AC Motors*

There are four AC motors that are competitive for the 19-52 Megawatt (MW) naval propulsion markets [3]. The motor types include: 1) Field Wound Synchronous Machines (FWSM), 2) Squirrel Cage Induction Machines (SCIM), 3) Permanent Magnet Synchronous Machines (PMSM), and 4) High Temperature Superconducting AC Synchronous Machines (HTSAC) [3]. The SCIM, PMSM, and HTSAC motors will be discussed and their qualities and shortcomings will be compared. The size and weight of the FWSM prohibits its use in surface combatants [3]. For this reason, the FWSM will not be examined in detail.

#### *b. DC Motors*

The Navy began researching Superconducting DC Homopolar Motors (SDCHM) in the early 1980's when an SDCHM homopolar motor was successfully demonstrated on the test craft *Jupiter II.* SDC homopolar motors will be discussed in detail in Chapter VI.

Other DC motors are not being widely considered because of a lack of available brush and slip-ring technology. Additionally, DC motors require a significant amount of maintenance on their brushes, which further deters their use in shipboard propulsion applications [4].

## D. POWER GENERATION AND DISTRIBUTION

### 1. Segregated and Integrated Power Systems

#### *a. Segregated Power System*

Currently, all U.S. Navy surface ships employ a segregated power system to provide electricity to various systems on the ship including propulsion, weapons and ship services. In a segregated power system, there are separate prime movers that provide propulsion power and ship service power. For example, in the DD-963 and the CG-47 classes of surface combatants, four large gas turbine engines are used strictly for propulsion. Three smaller gas turbine engines are used for electric power generation. Power is distributed throughout the ship via large switchboards and busses. The segregated power system requires seven prime movers to provide propulsion and auxiliary power.

#### *b. Integrated Power System (IPS)*

The Navy plans to use an IPS in future electric ships that will provide electric power for propulsion, weapons, and ship services. An IPS can reduce the number of installed prime movers from seven to four or less. By using a network of distribution busses and switching, an IPS can ensure that vital systems receive electric power in casualty situations. The IPS will provide the ability to rapidly reconfigure the electrical distribution system in the event of a combat equipment casualty. Figure 1 provides a comparison of the segregated and integrated power systems. The figure demonstrates the reduction of installed prime movers in the IPS as compared to the segregated system.

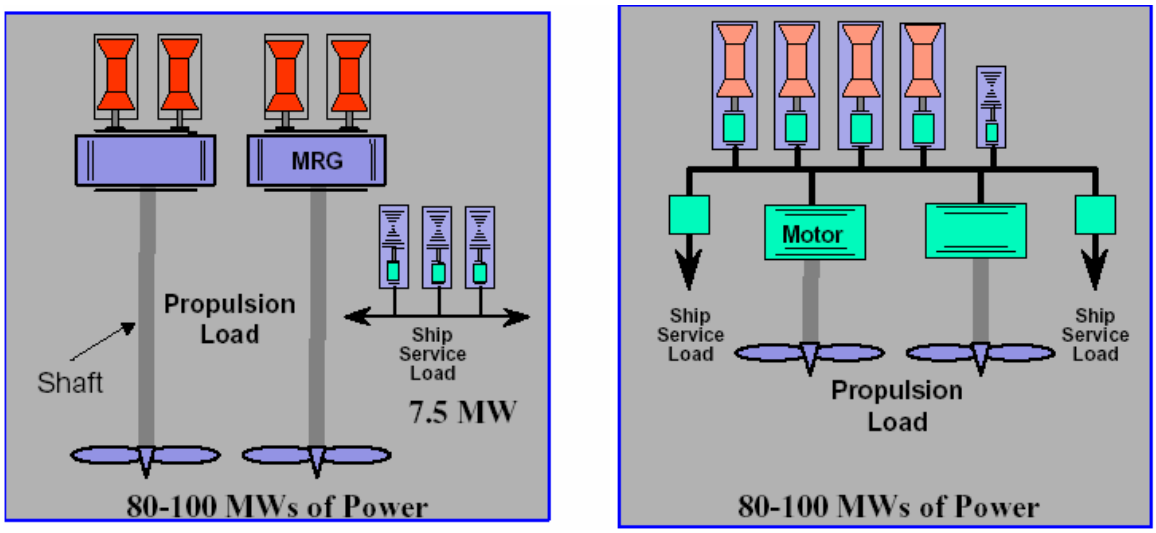


Figure 1.1. Comparison of the segregated and integrated power systems (From Ref. 5.)

## E. BENEFITS OF RETURNING TO ELECTRIC PROPULSION

The benefits of integrated systems include the unlocking of propulsion power [2], a reduction in the number of installed prime movers, increased fuel savings and improved design flexibility [6]. Performance benefits achievable through the use of electric propulsion include increased survivability and reliability, and reduced maintenance and manning requirements [6].

### 1. The Unlocking of Propulsion Power

The primary reason for implementing electric propulsion is the ability to unlock propulsion power for other uses [2]. Current ship designs do not fully employ the 80-100 MW of installed power. With electric propulsion and an IPS, power that is not used for propulsion can be used for other purposes such as high-powered pulsed weapons.

### 2. Cost

#### *a. Fuel Cost*

Significant fuel savings can be realized through the use of an IPS and electric drive. Estimates predict that there will be fuel savings of approximately 25 percent depending on which ship is used for comparison [7]. For example, industry data show that DD(x) outfitted with advanced gas turbine engines, IPS and electric drive systems will, on the average, cost approximately $80 million less per ship for fuel throughout its service life than the Navy's Arleigh Burke-class (DDG-51) destroyer [7]. With thirty-two ships planned, the fuel savings over the class lifecycle will be $2.56 billion, which is enough to purchase three additional ships [7]. These estimates may not solely be based on a reduction of installed prime movers but may also include the hydrodynamic efficiency benefits of podded propulsors [2].

#### *b. Manpower Costs*

Shipboard propulsion equipment requires a great deal of care and maintenance for its safe and proper operation. Reducing the amount of installed equipment reduces manpower requirements and therefore cost. Additionally, a great deal of automation is possible with the IPS, which will further reduce manning levels. Estimates predict that IPS and electric drive can reduce manpower levels by up to two-thirds [7].

### 3. Design Flexibility

The ubiquitous mechanical gas turbine propulsion system occupies an enormous amount of ship volume. This type of system is very large and allows little design flexibility. Gas turbine systems also require a great deal of auxiliary systems and equipment in order to function properly. Auxiliary equipment includes hydraulics, compressed air, cooling, shafts, shaft bearings, and shaft seals. Reducing the amount of auxiliary equipment frees up ship volume, which can be used for weapons, sensors, or crew comfort. Eliminating the need for separate generators for the production of electrical power frees up additional volume. Electric prime movers allow additional flexibility because copper cabling is less restrictive than a shaft arrangement. This allows ship designers to locate propulsion motors in such a way that optimizes the use of ship volume. Reducing restric-

tions on equipment placement during the shipbuilding process increases design flexibility.

#### 4. Survivability and Reliability

Electric propulsion and the modularity of the IPS will increase ship survivability and reliability by providing rapid isolation and redistribution of vital electric power during casualty situations. To meet survivability and reliability requirements, the ship service distribution system will use a zonal architecture that will provide redundancy in emergency situations [8]. Additionally, electric propulsion is expected to reduce noise, vibration, and heat signatures, thereby increasing the ship's ability to avoid detection by enemy forces [8]. These benefits are achievable through the use of fewer prime movers and the elimination of much of the hardware associated with a mechanical drive.

## F. ELECTRIC MOTOR FUNDAMENTALS

Rotating machines operate through the interaction of magnetic fields in the stationary and rotating portion of the machine. Torque is produced in the machine when the magnetic fields try to align with one another. This section is intended to provide a review of the basic construction and operation of rotating machines. For simplicity, three-phase machines will be discussed, although a shipboard propulsion motor is likely to contain more than three phases.

#### 1. Stator Construction

The stator is the stationary part of an AC machine. Synchronous and induction motor stators are alike. A simple three-phase stator is constructed by using three separate coils of wire each spaced 120° apart. Exciting the stator windings with a three-phase set of currents produces a rotating magnetic field of constant magnitude. Normal AC machine stators consist of several coils of copper wire in each phase, distributed in slots around the inner surface of the stator [9]. Figure 1.2 shows an AC machine stator with preformed stator coils.

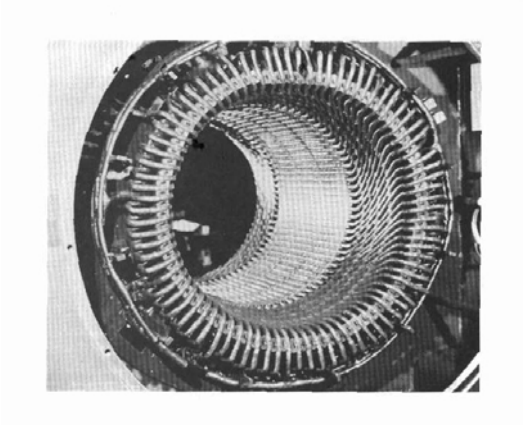

Figure 1.2. An AC motor stator with preformed stator coils (From Ref. 9.)

## 2. Rotor Construction

### *a. Induction Motor*

Induction motors have either wound rotors or squirrel cage rotors.

(1) Wound Rotor. Wound rotors are constructed using the same principle as stator construction.

(2) Squirrel Cage Rotor. The SCIM rotor has conducting bars embedded in grooves that are etched in the surface of the rotor along the direction of the rotor axis [9]. The conducting bars are placed around an iron core. To allow current flow in the bars, the bars are shorted at either end of the rotor by large shorting rings [9]. Squirrel cage rotor construction is shown in Figure 1.3. The rigid construction of this type of rotor contributes significantly to the robustness of the SCIM.

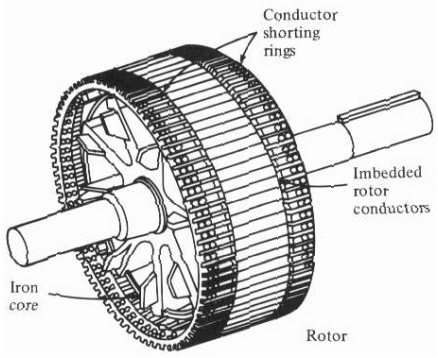


Figure 1.3. Squirrel cage rotor construction (From Ref. 9.)

### *b. Synchronous Motor*

Synchronous motors have either wound rotors or permanent magnet rotors. Figure 1.4 compares the two types.

(1) Field Wound Rotor. Field wound rotors are of the salient pole type. Salient pole rotors are constructed of protruding pole assemblies bolted or dovetailed to a magnetic rotor hub [10]. The rotor poles are wound with magnetic wire to produce a rotor magnetic field [10]. This type of construction requires an external circuit for field excitation. The FWSM is appropriate for large vessels such as icebreakers and auxiliary ships but its large size and weight make it unacceptable for use in surface combatants [3].

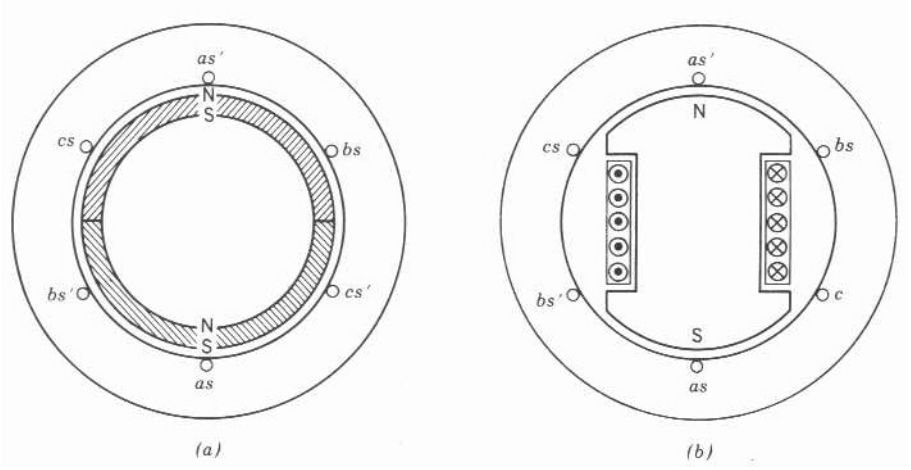


Figure 1.4. Structure of synchronous motors: (a) permanent magnet rotor (two-pole); (b) salient-pole rotor (two-pole) (From Ref. 13.)

(2) Permanent Magnet Rotor. Permanent magnet rotors receive their field excitation from permanent magnets mounted around the surface of the rotor instead of from field windings. A major advantage of PM synchronous motors is that slip ring or brushless exciter assemblies are not required [10]. This eliminates excitation losses, which are a major power loss component in field wound motors [10].

## G. CHAPTER I CONCLUSION AND THESIS OVERVIEW

Chapter I has introduced the Navy's Electric Ship Program and IPS and has presented many of the benefits of implementing an IPS. The electric motors currently being investigated for possible employment have also been introduced. The propulsion options that have been considered for use in future ship designs were introduced and they included in-hull propulsion and podded propulsion. Rotating machinery fundamentals were presented as a primer for the discussion of the various motor types that follows.

This thesis will examine the various motors being researched for propulsion applications. The properties, advantages and disadvantages of each motor and their associated drives will be compared. The current technology status of each motor will also be presented. Results from the Navy's IPS test platform will be presented and analyzed. The properties and benefits of using pods will also be investigated. Finally, a hypothetical 30 MW propulsion motor and its associated controller are modeled using MATLAB. Chapter II will examine the induction motor and discuss its properties and the current status of induction motor technology.

THIS PAGE INTENTIONALLY LEFT BLANK

# II. AC INDUCTION MOTORS

## A. INTRODUCTION

AC induction motors are the most employed electric machines in the world today. Induction motors are used extensively in industry and in households because of their low cost and rugged construction. One of the major advantages of the induction motor is its mechanical simplicity. The simple and rugged construction of the induction motor contributes to its reliability and makes it attractive for shipboard propulsion applications. There are two types of induction motors, the Squirrel Cage Induction Machine (SCIM) and the Field Wound Induction Machine (FWIM). This chapter discusses the operational properties of the SCIM. The large size of the FWIM prohibits its use as a ship propulsion motor, so it will not be discussed.

## B. THEORY OF OPERATION

### 1. Torque Development

The name induction motor arises from the nature of the developed torque [11]. Torque is developed when voltage is applied to the stator and current begins to flow in the stator windings. The stator winding currents produce a magnetic field that rotates in a counterclockwise direction. The changing magnetic field of the stator induces Electro Motive Forces (EMF) in the rotor cage winding. The induced EMF causes current flow and Magneto-Motive Forces (MMF) in the rotor windings. In turn the rotor MMFs produce a magnetic flux pattern, which also rotates in the air gap at the same speed as the stator-winding field [11]. The speed of rotation of the magnetic field is termed synchronous speed and it is given by [9]:

$$n_{sync} = \frac{120 f_e}{p} \tag{2-1}$$

where $f_e$ is the excitation frequency in Hz and $p$ is the number of poles in the machine. The rotating magnetic field, $\boldsymbol{B_S}$, passes over the rotor bars or windings and induces a voltage in them and causes rotor current to flow. The rotor current flow produces a rotor magnetic field $\boldsymbol{B_R}$ [9]. The torque induced by the two magnetic fields is given by [9]:

$$\tau_{ind} = k\mathbf{B}_R \times \mathbf{B}_S. \tag{2-2}$$

The value of *k* in Equation 2-2 is a constant that depends on the system of units used to express $\boldsymbol{B_R}$ and $\boldsymbol{B_S}$ [9]. Since the induced torque is in the counterclockwise direction, the rotor accelerates in the counterclockwise direction. The rotor can be accelerated to a speed at which the electromagnetic torque is balanced by the load torque [11]. When the load torque balances the electromagnetic torque, the motor's speed becomes steady.

### 2. Slip

The voltage induced in a rotor bar depends on the speed of the rotor relative to the magnetic fields. Slip is the term that is used to describe the relative motion of the magnetic fields and the rotor. Slip is expressed on a percent basis by the following equation [9]:

$$S[\%] = \frac{n_{sync} - n_m}{n_{sync}} \cdot 100\% \tag{2-3}$$

where $n_{sync}$ is the rotational speed of the magnetic field and $n_m$ is the rotor speed. Equation 2-3 assumes a two-pole machine. For a *p*-pole machine, Equation 2-3 becomes:

$$S[\%] = \frac{(2/p)n_{sync} - n_m}{(2/p)n_{sync}} \cdot 100\%. \tag{2-4}$$

Notice that if the rotor were to turn at synchronous speed, $s = 0$; while if the rotor is stationary, $s = 1$. All normal motor speeds fall somewhere between those two limits [9].

### 3. Induction Motor Losses

Ideally, ship propulsion motors should operate with the smallest value of slip possible. This is due to the fact that the rotor copper losses are equal to the air-gap power times the slip [9]. This relationship is given by the following [9]:

$$P_{RCL} = sP_{AG} \tag{2-5}$$

where $P_{RCL}$ is the rotor copper loss, $s$ is the slip and $P_{AG}$ is the air-gap power. Losses in the induction motor have a negative affect on the efficiency and therefore need to be minimized. Efficiency is given by [9]:

$$\eta[\%] = \frac{P_{out}}{P_{in}} \cdot 100\% \tag{2-6}$$

where $\eta$ is the efficiency, $P_{out}$ is the output power, and $P_{in}$ is the input power.

The $I^2R$ losses are the first losses encountered in the induction motor and they occur as stator copper loss $P_{scl}$ [9]. Power is also lost in the stator in the form of hysteresis and eddy currents. These are considered core losses, $P_{core}$ [9]. The power remaining is transferred to the rotor of the machine through the air-gap between the stator and the rotor [9]. After the power is transferred to the rotor, some of it is lost in the form of $I^2R$ losses, $P_{RCL}$ [9]. Other losses in the machine include friction and windage losses, $P_F$ and $P_W$ respectively [9], and stray magnetic losses. The output power $P_{out}$ is found by subtracting the machine's losses from the input power, $P_{in}$.

## C. TECHNOLOGY DEVELOPMENT

### 1. Advanced Induction Motor

Improvements in induction motor technology over the last several years have made induction motors ideal candidates for ship propulsion applications. Alstom Corporation's Advanced Induction Motor (AIM) has been evolving over the past 15 years [12]. It was primarily developed for applications where low speed and high torque are required, such as in ship drives [12]. The AIM has a very high power density that makes it ideal for warship propulsion where space is at a premium [12]. The AIM was selected in 1995 for the U.S. Navy's IPS program and it was selected to be the primary propulsion motor for the next generation of U.K. warships, the Type-45 destroyer [12]. This section discusses some of the important properties of the AIM that make it ideal for propulsion applications.

### 2. Power Density

In applications requiring a low-speed, high-torque drive, the design of the induction motor can be optimized to increase the power density without any penalties in performance [12]. The Air Gap Shear Stress (AGSS) is one measure of power density in an

induction motor [12]. The AGSS is the force per unit area on the rotor surface due to the motor torque and is given by [12]:

$$\sigma_g = \frac{\tau}{2\pi r_r^2 l_r} \tag{2-7}$$

where $\sigma_g$ is the AGSS, $\tau$ is the motor torque, $r_r$ is the rotor radius, and $l_r$ is the rotor core length [12]. Power density has been increased in the AIM through optimizing the electromagnetic design of the rotor [12]. Equation 2-7 indicates that the torque produced by an induction motor is directly proportional to the magnetic forces. Optimizing the electromagnetic forces increases torque and the AGSS. Table 2.1 provides a comparison of the AGSS of the AIM with other motor technologies. Note that the AIM AGSS is approaching that of the permanent magnet synchronous motor, which is described in the next chapter [12].

| **Motor** | **Airgap Shear Stress ($kNm^{-2}$)** |
|---|---|
| Standard large industrial induction motor | 13 |
| High performance industrial 1500 rpm induction motor | 35 |
| Low speed mill motor (origins of the AIM) (1992) | 45 |
| IPS Motor for US Navy, 19 MW at 150 rpm, (1997) | 76 |
| Current AIM design, 20 MW at 180 rpm, (2002) | 100 |
| Permanent Magnet Motor | 120 |
| High Temperature Superconducting Motor, 25 MW at 120 rpm | 340 |

Table 2.1. Air gap shear stress comparison (From Ref. 12.)

### 3. Motor Cooling

High power-density motors must have an efficient method in place for cooling. Alstom's AIM is fundamentally an air-cooled machine, but can use an air/water heat exchanger when required [12]. The AIM uses stator and rotor core construction incorporating radial ventilation ducts that are provided using a patented Alstom method known as "pin-vent" [12]. The pin vent method provides an efficient way of removing heat from the windings [12].

### 4. Signature Reduction

Noise signature reduction is obviously an important consideration in warship propulsion. A standard induction motor is not normally regarded as suitable where a low noise signature is required, since the combination of a slotted stator and rotor together with a small air gap produce significant levels of force on the stator teeth and, hence, high noise levels [12]. In order to reduce noise levels, the forces that are responsible for producing the noise need to be reduced. Electromagnetic forces in the AIM are reduced by selecting the appropriate number of stator and rotor slots, poles, and phases [12]. This minimizes the number and amplitude of forcing frequencies [12]. Further noise reduction is possible through advanced structural dynamics and mounting methods. The structural dynamics of the AIM and its mounting structure are designed to provide minimal noise transmission [12].

In a ship propulsion application in steady state operation, the power required by the propeller is proportional to the speed cubed [12]. Since a ship spends much of its time operating at less than 50% full power, additional noise signature improvements can be achieved by taking advantage of this cubic power dependence [12]. Also, decreasing the quantity of cooling air at reduced speed and power can reduce ventilation noise [12]. An optimized strategy for motor flux control is employed at reduced speed to minimize electromagnetic noise [12]. Further noise reduction is possible through the careful selection of an appropriate converter for the drive. This is discussed in a later chapter.

### 5. Shock Performance

Compared to other types of rotating electrical machines, an induction motor is inherently robust [12]. The rotor in the AIM is of simple construction, with solid copper conductors. The conductors are contained in slots in an iron core without the use of insulation [12]. AIM designs have been qualified to US Navy and Royal Navy shock standards [12].

### 6. Cost

Since the SCIM has a very simple design and is inherently robust, it is less expensive than a similarly rated PMSM. The SCIM is approximately 15% less expensive than the PMSM [3].

### 7. Size and Weight

The SCIM is roughly the same size as an equally rated PMSM, but it is much lighter. A 20 MW, 6-pole, 6-phase machine weighs approximately 80 tons whereas a comparatively sized PMSM weighs approximately 100 tons.

## D. CHAPTER II CONCLUSION

This chapter has introduced the induction motor, its theory of operation, and some of its physical properties that make it suitable for ship propulsion. The current status of induction motor development was presented with the discussion of Alstom's AIM. The AIM has been demonstrated in the U.S. Navy's IPS program (described in Chapter VII), and the U.K. Royal Navy selected it for use in the Type-45 destroyer. Although the AIM has been proven to be ideal for ship propulsion, work is ongoing to develop the PMSM for ship propulsion. Permanent magnet motors are expected to have significant advantages in size and weight as compared to conventional wound motors [3]. Chapter III discusses the PMSM and the current status of its development.

# III. AC SYNCHRONOUS MOTORS

## A. INTRODUCTION

Synchronous motors are widely used in commercial shipping, large auxiliary ships, and cruise liners. This includes both the FWSM and the PMSM. The PMSM has received favorable consideration as a ship propulsion motor because of its power density and quiet operation. The U.S. Navy is currently planning to use the PMSM to provide propulsion for the DD(x). This chapter discusses basic PMSM motor theory, the different types of PMSM, their physical properties, and the current status of PMSM technology development. The FWSM is too large for use in a surface combatant, so it will not be discussed in this chapter.

## B. THEORY OF OPERATION

### 1. Basic Operating Principles

Synchronous motors operate on the same basic phenomenon as induction motors. The main difference is that the rotor magnetic field is not induced, but rather is provided by an external excitation circuit in a field wound motor or a magnet in a permanent magnet motor. The description that follows is based on a permanent magnet motor.

#### *a. Torque Development*

Torque is produced in an AC synchronous motor in the same manner that it is produced in an induction motor. Torque results from the interaction of two magnetic fields. Stator currents produce a magnetic field in the stator that interacts with the field from the permanent magnets on the rotor. When the two fields try to align, torque is produced and the machine turns.

#### *b. Magnetic Flux and Induced EMF*

The operation of the synchronous motor is possible due to the magnetic flux produced by the permanent magnet and the induced EMF in the stator winding. The permanent magnet on the rotor produces a flux $\phi_f$ in the air gap. The flux rotates at synchronous speed, $\omega_s$ rad/s, which is the same as the rotor speed [13]. The flux $\phi_{fa}$ linking one of the stator phase windings, for example phase *a*, varies with time [13]:

$$\phi_{fa}(t) = \phi_f \sin \omega t \tag{3-1}$$

where

$$\omega = 2\pi f = \frac{p}{2}\omega_s \tag{3-2}$$

and $p$ is the number of poles in the motor [13]. Assuming that $N_s$ is an equivalent number of turns in each stator phase winding, the emf induced in phase *a* is [13]

$$e_{fa}(t) = N_s \frac{d\phi_{fa}}{dt} = \omega N_s \phi_f \cos \omega t. \tag{3-3}$$

The induced voltage in the stator winding is the excitation voltage and its rms value is

$$E_{fa} = \frac{\omega N_s}{\sqrt{2}} \phi_f. \tag{3-4}$$

In accordance with normal convention, the amplitudes of voltage and current phasors are represented by their rms values and the amplitudes of flux values are represented by their peak values [13]. Representing $e_{fa}$ and $\phi_{fa}$ as phasors at $\omega t = 0$ with $E_{fa}$ being the reference phasor in Figure 3.2:

$$\overline{\phi_{fa}} = -j\phi_f, \tag{3-5}$$

$$\overline{E_{fa}} = j\frac{\omega N_s}{\sqrt{2}}\overline{\phi_{fa}} = E_{fa}. \tag{3-6}$$

The frequency of the voltage applied to the stator of a synchronous motor is [13]:

$$f = \frac{p}{4\pi}\omega_s. \tag{3-7}$$

The fundamental frequency components of these stator currents produce a constant amplitude flux $\phi_s$ in the air gap that rotates at synchronous speed [13]. The amplitude of $\phi_s$ is proportional to the amplitudes of the fundamental frequency components in the stator currents [13].

Figure 3.1 shows the phasor diagram corresponding to the quantities discussed herein. Also shown in Figure 3.1 is the synchronous motor equivalent circuit (one phase). Figure 3.1 should be referred to in the description that follows.

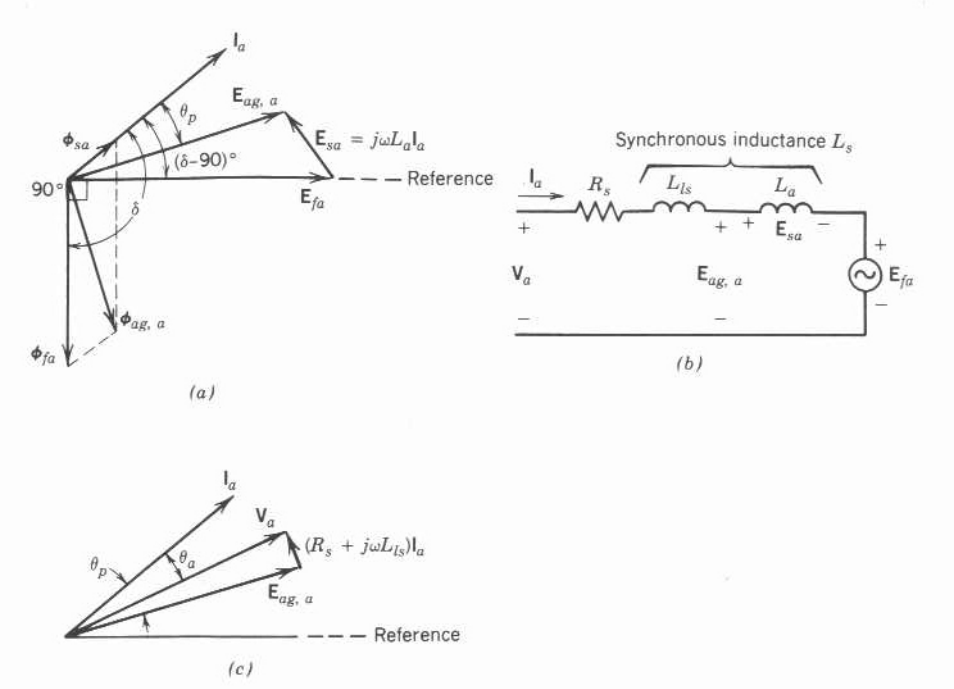


Figure 3.1. Per-phase representation: (a) phasor diagram; (b) equivalent circuit; (c) terminal voltage (From Ref. 13.)

The flux linking with phase *a* due to $\phi_s$ produced by all three stator currents is $\phi_{sa}(t)$ [13]. This flux is proportional to the phase a current $i_a(t)$ [13] (see Figure 3.1):

$$N_s \phi_{sa}(t) = L_a i_a(t). \tag{3-8}$$

The voltage induced in phase *a* due to $\phi_{sa}(t)$ is from Equation 1.19:

$$e_{sa}(t) = \frac{N_s d\phi_{sa}}{dt} = L_a \frac{di_a}{dt}.$$

If we assume that the fundamental component of the supplied current to the stator phase *a* is [13]:

$$i_a(t) = \sqrt{2} \cdot I_a \sin(\omega t + \delta), \tag{3-9}$$

then the induced voltage in phase *a* is [13]:

$$e_{sa}(t) = \sqrt{2} \cdot \omega L_a I_a \cos(\omega t + \delta) \tag{3-10}$$

where δ is the torque angle [13]. Representing $i_a$ and $e_{sa}$ as phasors [13]:

$$\overline{I_a} = I_a e^{j\left(\delta - \frac{\pi}{2}\right)}, \tag{3-11}$$

$$\overline{E_{sa}} = j\omega L_a \overline{I_a} = \omega L_a I e^{+j\delta}. \tag{3-12}$$

The air-gap flux linking the stator phase *a* is the sum of $\phi_{fa}(t)$ and $\phi_{sa}(t)$, which can be written in phasor form as [13]:

$$\overline{\phi_{ag,a}} = \overline{\phi_{fa}} + \overline{\phi_{sa}}. \tag{3-13}$$

The air-gap voltage due to the air-gap flux in phasor form is [13]:

$$\overline{E_{ag,a}} = \overline{E_{fa}} + \overline{E_{sa}} = \overline{E_{fa}} + j\omega L_a \overline{I_a}. \tag{3-14}$$

All of the phasors mentioned above are drawn in Figure 3.1 (a) [13]. Also shown in Figure 3.1(b) is a per phase equivalent circuit of a synchronous motor where $R_s$ and $L_{ls}$ are the stator winding resistance and leakage inductance, respectively [13]. The per phase terminal voltage in phase *a* is [13]:

$$\overline{V_a} = \overline{E_{ag,a}} + (R_a + j\omega L_s)\overline{I_a}. \tag{3-15}$$

The phasor diagram corresponding to Equation 3-15 is shown in Figure 3.1(c), where $\phi_a$ is the angle between the current and terminal voltage phasors [13].

***c. Slip***

The term slip does not apply to synchronous motors as it did induction motors since the rotor turns at the same speed as the rotating magnetic field.

***d. Losses***

Synchronous motors experience the same losses that induction motors experience. Efficiency in the synchronous motor is improved by minimizing losses and by increasing the magnetic flux.

## C. TYPES OF PMSM

Permanent magnet synchronous motors can be placed in three different classes depending on the direction of the magnetic flux. The machine types are described below.

### 1. Axial Flux Synchronous Motor

The axial flux synchronous motor consists of a cylindrical magnetic rotor rotating within a cylindrical stator [3]. This motor has its flux direction parallel to the rotor shaft. Axial flux motors are coming into prominence because of their higher power density and acceleration [14]. Higher power density is achieved by effectively doubling the number of air gaps in a given volume [3]. This ability makes this type of motor much lighter than a comparable FWSM [3]. Another advantage of this type of machine is that it offers a modular construction where multiple rotors and stators can be placed together in stages to achieve a multi-stage machine arrangement [14]. Figure 3.2 shows the basic layout of an axial-flux motor. Another advantage of the machine shown in Figure 3.2 is that the stator winding end lengths are very short. This is an advantage because no useful torque is produced from the end windings. Figure 3.3 provides the basic layout of a 4-stage axial flux machine. The figure illustrates the modular architecture that is possible with this type of machine.

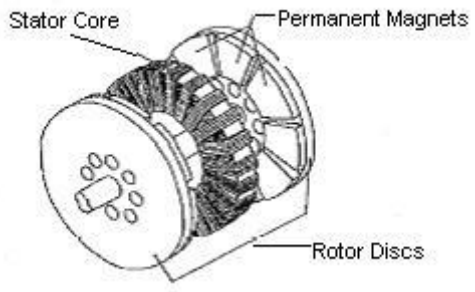


Figure 3.2. Basic layout of an AFPM machine (After Ref. 15.)

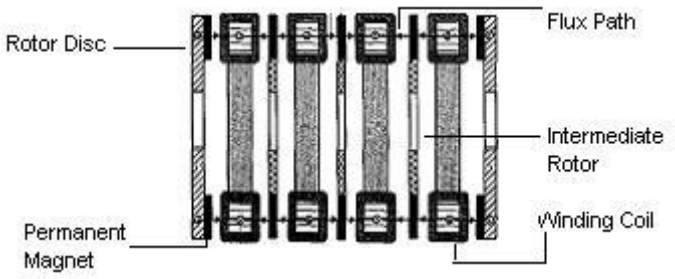


Figure 3.3. Cross-sectional side view of a 4-stage AFPM (After Ref. 15.)

### 2. Radial Flux Synchronous Motor

Radial flux flow is the traditional and conventional operating principle for rotating electric machines [16]. The radial flux synchronous motor consists of a cylindrical rotor that rotates within a cylindrical stator [3]. This type of motor has a flux direction that is along the radius of the machine. The radial flux machine is shown in Figure 3.4. Note that the machine in Figure 3.4 has salient pole construction and an on-shaft exciter [9].

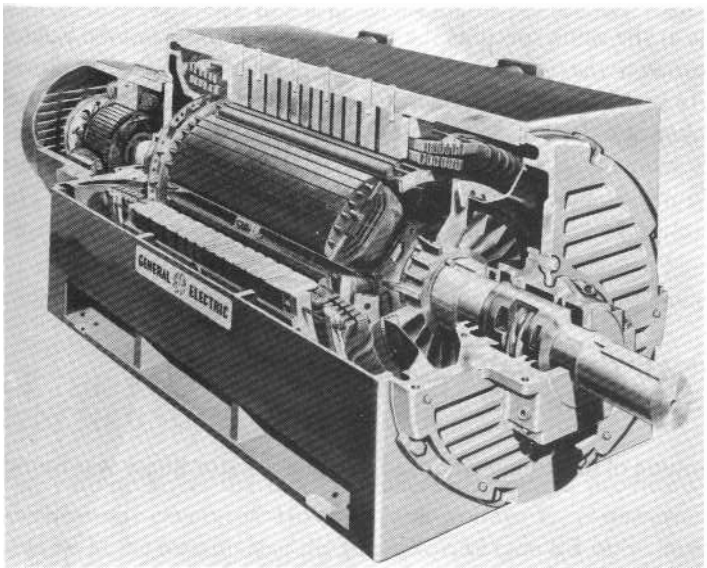


Figure 3.4. Cutaway diagram of a large synchronous motor (From Ref. 9.)

### 3. Transverse Flux Synchronous Motor

Transverse flux synchronous motors are made up of a rimmed disk that spins between slotted rings [3]. The motor is configured with a disk that has N-S magnets lined up around the periphery [3]. Stator coils run coaxial with the rotor with the stator winding flux linking the PM flux through a series of stator hoops [3]. An advantage for this type of machine is that it can produce useful torque at both the inner and outer surfaces of the rotor [3]. The transverse flux machine is illustrated in Figure 3.5. The N-S magnets and the stator hoops are clearly visible in the figure.

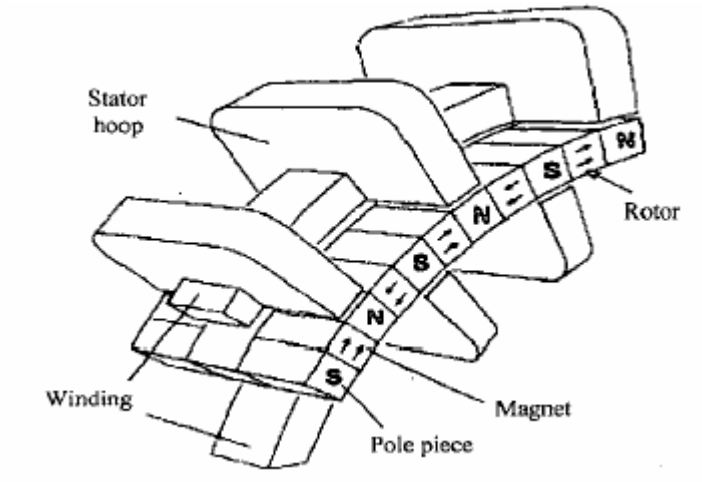


Figure 3.5. Illustration of the transverse flux machine concept (From Ref. 17.)

## D. TECHNOLOGY DEVELOPMENT

### 1. Axial Flux

Kaman Aerospace Corporation is developing this type of motor in the U.S [18]. They have proposed a 19 MW design consisting of 32 phases, each with a 600 kW inverter [3]. The estimated weight of the drive was 50,000 kg versus a comparable FWSM weight of 229,000 kg [3]. Jeumont Industrie is also developing this motor in France [19]. Table 3.1 compares the Jeumont Industrie motor with a conventional wound motor. As the table indicates, significant weight reductions are possible with the axial flux machine.

| | Overall weight | External diameter | Overall length |
|---|---|---|---|
| Axial field magnet motor | 65 tonnes | 2.7 m | 3.0 m |
| Wound synchronous motor | 120 tonnes | 5.6 m | 3.6 m |

Table 3.1. Comparison of Jeumont Industrie motor with a conventional wound synchronous motor (From Ref. 19.)

### 2. Radial Flux

Jeumont Industrie is promoting radial flux motor development in France. They have successfully demonstrated a 1.8 MW machine that is made using SmCo for the permanent magnets [3]. Kaman Aerospace and General Dynamics Marine Division are also pursuing additional efforts in radial flux technology [3].

### 3. Transverse Flux

Rolls Royce corporation is developing a 20 MW 180 RPM Transverse Flux Motor (TFM) for the U.K. Ministry of Defense (MOD) for possible employment in surface combatants [19]. The power factor for this motor is currently anticipated to be 0.6 [19]. This relates to an air-gap shear stress of 100 $kN/m^2$; however, the machine could be designed for an air-gap shear stress of 120 kN/m2, but with a consequent reduction in power factor to 0.4 [19]. With a power factor of 0.4, the motor would require a 50 MVA converter [19]. This reduces the efficiency of this type of motor because of the increased switching and conduction losses [19]. The TFM topology has a greater potential for torque density than is currently being exploited in the MOD development [19]. Torque density is currently limited by the available converter technology.

## E. CHAPTER III CONCLUSION

This chapter has introduced the PMSM, its advantages, and the current status of its development. Three types of PMSM were introduced and their properties and benefits were discussed. Permanent magnet motors are being developed and improved because of their potential increase in power density. Using High Temperature Superconducting (HTS) wire in motor construction can increase power density much more. HTS motors will be the focus of Chapter IV.

THIS PAGE INTENTIONALLY LEFT BLANK

# IV. HIGH TEMPERATURE SUPERCONDUCTING AC SYNCHRONOUS MOTOR

## A. INTRODUCTION

Advances in High Temperature Superconductors (HTS) are enabling a new class of synchronous rotating machines that can be generically categorized as super machines [20]. These super machines include both motors and generators. HTS motors are expected to be less expensive, lighter, more compact, and more efficient than similarly rated conventional machines [20]. The motors will also be more power dense than conventional motors because of the increased current carrying capacity in the HTS stator wires. When fully developed and employed, these motors will drastically reduce the amount of ship volume consumed by propulsion motors. This chapter will discuss the background and properties of superconducting wire and HTS motors, their benefits, and the current progress being made in their development.

## B. SUPERCONDUCTING TECHNOLOGY BACKGROUND

### 1. Low Temperature Superconducting Wire (LTS)

Superconducting wire in its Low Temperature Superconductor (LTS) form has been in widespread use for over 30 years [20]. Some of the commercial applications for LTS wire include high-powered particle accelerators and Magnetic Resonance Imaging (MRI) systems for the medical field [20]. During the 1970's, General Electric (GE) and Westinghouse conducted generator design studies that were based on LTS wire [20]. GE also built and tested a 20 MVA superconducting generator in the 1970's [20]. The Navy built and tested a superconducting DC homopolar motor in the early 1980's that used LTS wire. During the 1990's, a Japanese consortium built and tested a 70 MW generator [20]. Niobium Titanium alloy (NbTi) LTS wire was used in all of the aforementioned machines [20].

#### *a. The Problem with LTS Wire*

When a superconductor's temperature exceeds its operating level, quenching can result. Quenching occurs when a superconducting material loses its superconducting properties. Quenching is governed by the magnetic field, current density, and

operating temperature. An increase in magnetic field, temperature, or current density can cause quenching. In order to prevent quenching, LTS wire has to be operated at a very low temperature of 4K, which requires very expensive and complex cooling equipment [20]. The cost and complexity of such cooling equipment has prevented further development of LTS superconducting motors for propulsion applications.

### 2. HTS Wire

The discovery of High Temperature Superconductors in 1986 added promising prospects to the possibility of commercializing superconducting industrial motors [21]. HTS wire technology has been advancing over the past 17 years, which has resulted in superconducting magnets that can operate at substantially higher temperatures than LTS magnets [20]. HTS wires are made of Bismuth 2223 (Bi2223). The wires are much smaller than traditional copper wires and can handle current that is orders of magnitude larger than copper wires when kept at the right operating temperature. HTS wire is resistant to quenching because an HTS wire can absorb more heat energy than LTS wire without a drastic increase in its temperature. Also, unlike LTS wire, HTS wire loses its current carrying capacity gradually. This advantage makes it possible to use refrigeration and cooling systems that are less complex and less expensive [20].

## C. HTS MOTOR CONSTRUCTION

### 1. Stator Construction

Current HTS motor designs use conventional copper wire for stator construction. The stator of the 25 MW, 120-RPM HTS motor being developed by American Superconductor Corporation (AMSC) is made up of a 6.6-kV copper winding and is cooled with freshwater [20]. Although the stator is made up of conventional copper windings, there are a few differences in its construction. The stator winding is not housed in conventional iron core teeth because they saturate due to the high magnetic field imposed by the HTS winding [20]. Eliminating the iron core teeth and the vibration caused by them helps to reduce noise emissions from the motor.

### 2. Rotor Construction

The rotor windings in the ASC motor are made up of HTS wire and cooled with an off-the-shelf cryogenic cooler [22]. The HTS field was designed to operate in the 25–35 Kelvin temperature range with a DC magnetic field in the range of 2-4 Tesla [22].

### 3. Cryogenic Cooler

The HTS motor uses an off-the-shelf cryocooler system that feeds cold fluid to and receives warmed fluid from the rotor [22]. The cryocooler uses liquid nitrogen as the cooling medium. Cryogenic coolers do not present a significant risk in terms of equipment maintenance or failure. A defective cooler could be replaced in less than 30 minutes without having to stop the motor [20].

## D. HTS MOTOR DEVELOPMENT

Several companies are actively developing super machines including AMSC, Rockwell Automation, Siemens and GE [20]. A 1000 hp, 1800-rpm motor built by a team consisting of Rockwell Automation, AMSC, and others was successfully operated in May 2000 [20]. Siemens demonstrated a 550 hp, 1800-rpm motor in the summer of 2001 [20]. AMSC is currently under contract with the Office of Naval Research (ONR) to develop a 36 MW HTS motor for naval propulsion applications.

### 1. AMSC 25 MW HTS Motor

AMSC has conducted prototype testing if a 25 MW proof of concept propulsion motor. This section discusses the results of the prototype testing. The ONR design goals for the 25 MW motor are presented in Table 4.1. Table 4.2 provides the results of electric modeling of the 25 MW motor. Figure 4.1 shows the main features of the AMSC 25 MW motor.

| List of parameters | Value |
|---|---|
| Nominal Rating | 25 MW |
| Line Voltage | 4160 volt |
| Speed at full-load | 120 rpm |
| Efficiency at full load | >96% |
| Structureborne Noise | <60 dB |
| Design Life | 30 yrs |

Table 4.1. 25 MW motor goals (From Ref. 23.)

| List of parameters | Value |
|---|---|
| Number of Phases | 9 |
| Line Voltage | 4160 volt |
| Speed at full-load | 120 rpm |
| Phase current | 622 A |
| Load angle | 19.1 deg. |
| Synchronous Reactance | 0.34 pu |
| Transient Reactance | 0.275 pu |
| Subtransient Reactance | 0.19 pu |
| Overall Efficiency | 97.5% |
| Predicted full speed structureborne noise | 47 dB |

Table 4.2. 25 MW motor concept predicted performance (From Ref. 23.)

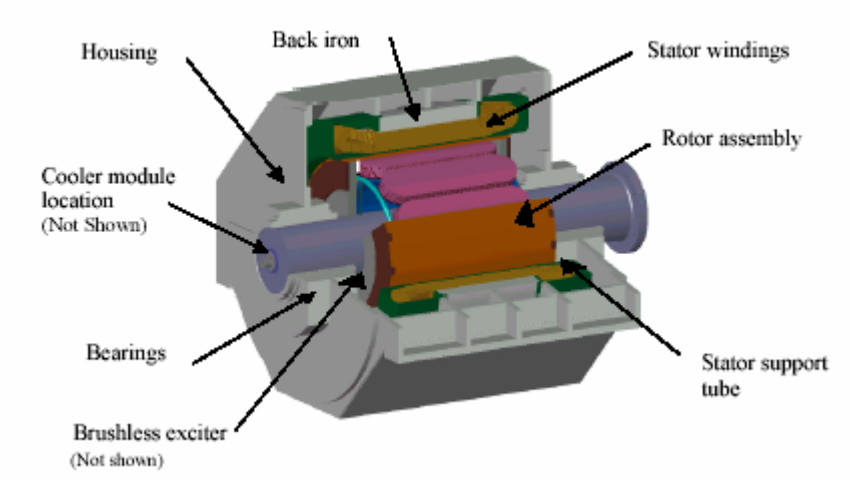


Figure 4.1. 25 MW, 120 RPM ship propulsion motor (From Ref. 23.)

### *a. Efficiency*

The ONR design goal was to have efficiency greater than 96%. Modeling produced an efficiency of 97.5% overall. The efficiency at part-load was also measured and found to be greater than 98%, as shown in Figure 4.2.

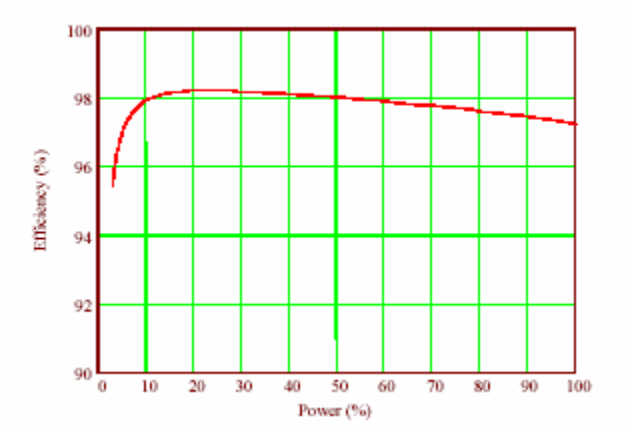


Figure 4.2. HTS motor efficiency at partial-load (From Ref. 23.)

### *b. Structure-Borne Noise*

As Tables 4.1 and 4.2 show, structure-borne noise emissions from the motor were well below the design goal of less than 60 dB. Since the machine has a high magnetic field, the size of the machine is reduced [23]. This causes greater forces to be exerted on the machine's back iron. The deflected and the predicted noise in the back iron are shown in Figure 4.3. Both the full speed and the ¾ speed back iron noise are provided. In both cases, the noise levels were lower than the design requirements.

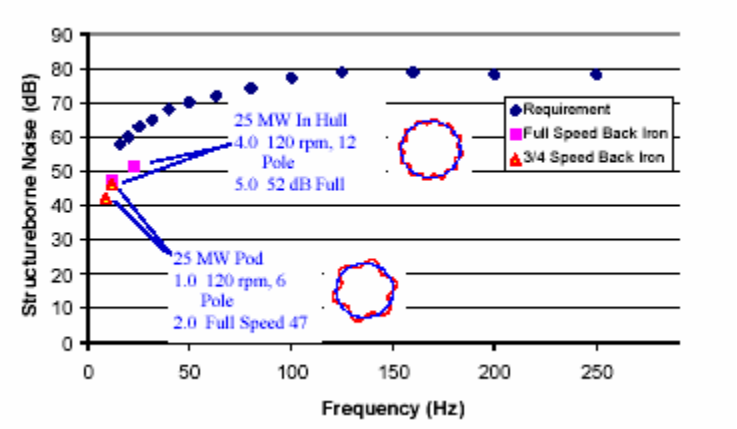


Figure 4.3. Structure borne noise prediction for 25 MW HTS motor (After Ref. 23.)

### *c. Size and Weight*

HTS motors are much more power dense than conventional motors and are therefore smaller and lighter. The 25 MW machine is estimated to be 2.5 m long and 2.4 m in diameter [23]. The machine has an estimated weight of 60-70 tons [23]. This represents a significant weight reduction when compared to the 117-ton weight of the 19 MW IPS Advanced Induction Motor.

### *d. Harmonic Performance*

Conventional motors typically have substantial $5^{th}$ and $7^{th}$ harmonics generated by the field in the armature and by the armature at the rotor surface [23]. As Figure 4.4 shows, the HTS motor harmonic content is nearly zero. This is due to the fact that the machine does not use saturated iron in the stator [23].

| Harmonic number | Generated by field in armature | Generated by armature at the rotor surface |
|---|---|---|
| 1 | 1 | 1 |
| 3 | $-7.527 \cdot 10^{-4}$ | 0.014 |
| 5 | $2.582 \cdot 10^{-3}$ | -0.01 |
| 7 | $-3.358 \cdot 10^{-5}$ | $2.502 \cdot 10^{-3}$ |
| 9 | $6.388 \cdot 10^{-6}$ | $7.892 \cdot 10^{-4}$ |
| 11 | $-8.983 \cdot 10^{-5}$ | $-4.332 \cdot 10^{-4}$ |
| 13 | $-1.494 \cdot 10^{-7}$ | $1.451 \cdot 10^{-4}$ |
| 15 | $-7.472 \cdot 10^{-6}$ | $1.149 \cdot 10^{-4}$ |
| 17 | $7.477 \cdot 10^{-6}$ | $-4.944 \cdot 10^{-5}$ |
| 19 | $1.865 \cdot 10^{-9}$ | $1.673 \cdot 10^{-5}$ |

Figure 4.4. Harmonics generated in armature and at rotor surface in the 25 MW motor (From Ref. 23.)

## E. CHAPTER IV CONCLUSION

Chapter IV has introduced superconducting wire and the advantages of HTS motors. A brief review of HTS motor development was given. Test results from a 25 MW prototype ship propulsion motor were presented and compared to design goals. The results indicated that efficiency and structure borne noise were well within the design goals. The size, weight and power density advantages of HTS motors were also discussed. HTS synchronous motors are sure to be employed whenever the technology is advanced

enough to do so. The HTS technology is not limited to synchronous machines. HTS wire can also be used in the development of a DC homopolar motor for ship propulsion, which is the focus of Chapter V.

THIS PAGE INTENTIONALLY LEFT BLANK

# V. SUPERCONDUCTING DC HOMOPOLAR MOTOR

## A. INTRODUCTION

The Homopolar machine was the first rotating electrical machine developed and was demonstrated by Michael Faraday in 1831 [24]. The U.S. Navy has been researching the SDCHM since the 1960's [3]. The homopolar machine concept has been investigated because of its ability to produce high and constant torque over a wide speed range [24]. Homopolar motors are attractive for potential use in direct electric drives for ships because of their compactness and high power density [25]. This chapter will introduce the SDCHM and discuss the Navy's experimental results. The current status of the technology will also be discussed.

## B. MOTOR CONSTRUCTION AND THEORY OF OPERATION

### 1. Machine Types

There are two types of SDCHM and they include the disk armature machine and the drum armature machine. The two machine configurations are presented conceptually in Figure 5.1 along with some of the benefits of the SDCHM.

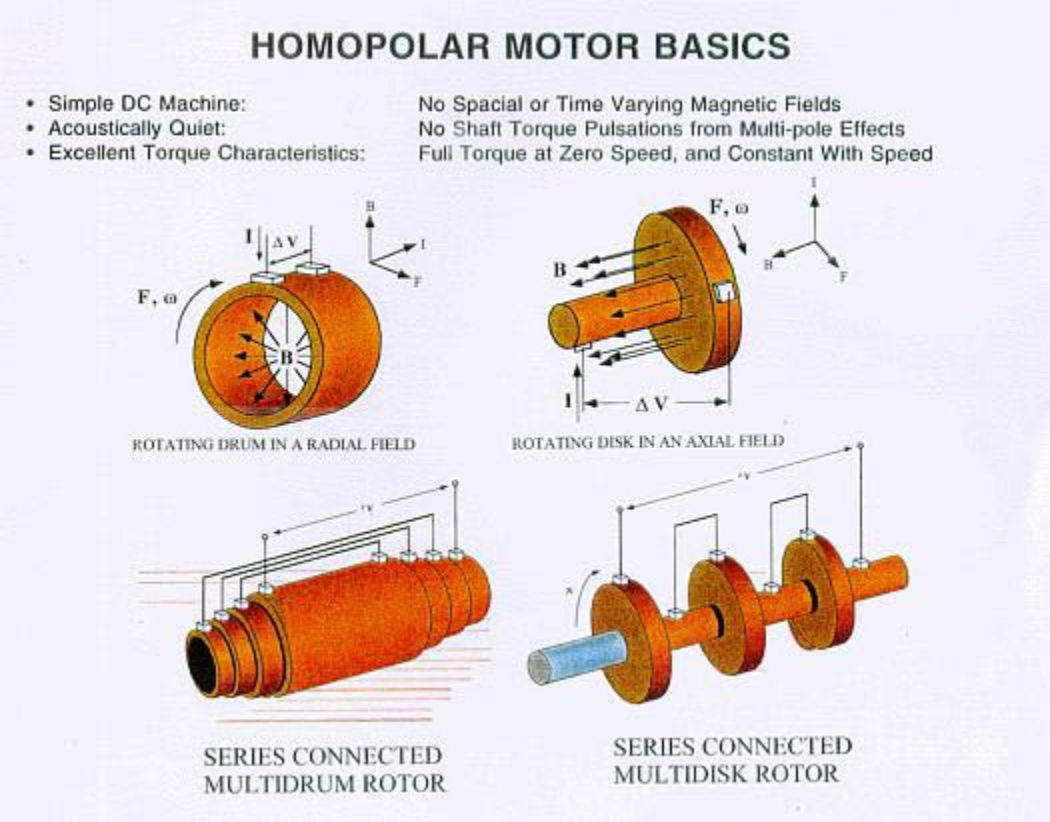


Figure 5.1. Homopolar motor design showing the disk and drum armature homopolar motor (From Ref. 26.)

### *a. Disk Armature Machine*

The disk armature machine in Figure 6.1 consists of an electrically conducting disk that is located in a uniform, axially directed magnetic field [24]. An electric current applied to the disk interacts with the axial magnetic field and develops a mechanical force that rotates the disk [24]. The developed force is based on Faraday's Law of Induction [24]:

$$\overline{dF} = I\overline{dL} \times \overline{B} \tag{5-1}$$

where $I$ is the current in the conductor, $\overline{B}$ is the magnetic field flux density through which the current flows, and $\overline{dL}$ is the circuit differential path length [24]. The forces developed in the armature and stator of the motor can be found by integrating $\overline{dF}$ around the circuit [24].

### *b. Drum Armature Machine*

A drum-type rotor that is located in a radial magnetic field will experience a rotational force when axial current flows through the drum [24]. For both motor configurations, the motor action is produced without changing the direction (polarity) of the magnetic field or the armature current of the machine [24].

### *c. Stator Construction*

The stator of the homopolar motor is constructed using HTS wire. The benefits of using HTS wire have already been presented and they include higher efficiency, smaller design, and higher power density.

## C. SDCHM ADVANTAGES

Because of the homopolar magnetic behavior, the field windings of the machine do not experience a mechanical torque in reaction to the armature torque [24]. The reaction torque is developed in the current-carrying conductors of the stator of the machine and not the field winding [24]. An added advantage of the homopolar motor is that when the magnitudes of $\overline{J}$ and $\overline{B}$ are constant in time (a DC machine), the force developed and transmitted by the shaft of the machine will be constant [24]. The constant current and field of the homopolar motor eliminates mechanical torque pulsations on the shaft. Eliminating the torque pulsations provides an acoustically quiet machine.

## D. NAVAL SURFACE WARFARE CENTER (NSWC) HOMOPOLAR MOTOR

The U.S. Navy conducted the first operational test of an SDCHM in 1980 aboard the NSWC test craft *Jupiter II* [24]. That motor used LTS wire. Since then, another homopolar motor has been tested using Bi 2223 HTS wire. This section describes some of the details relating to the construction of the latest NSWC homopolar motor.

### 1. Field Windings

The field winding of the NSWC homopolar motor was designed and constructed with magnets wound with Bi 2223 wire and cooled to a temperature of 4.2K with liquid helium [24]. The only superconducting component in the motor was the field winding. The field winding of the motor was arranged in a split, two-magnet configuration. Su-

perconducting windings were wound around each magnet. The two magnets were axially separated by a distance of 10.6 cm and were electrically connected so that their axial magnetic fields would be in flux opposition [24]. Details relating to the size, length and diameter of the field windings can be found in Reference 24. The benefits of employing HTS windings instead of LTS windings were presented in Chapter IV. This applies directly to the SDCHM. The SDCHM currently being explored by General Atomics is based on a design using HTS wire.

### 2. Armature Construction

The armature was a drum-type armature. Sodium potassium (NaK) liquid metal current collectors were used to transfer current between the stator of the machine and its rotating armature [24]. Liquid metal current collectors were used because they can operate at higher current densities, they are able to operate at higher rotational speeds, they have improved power conversion efficiencies, and they last longer than conventional solid brush current collectors [24]. The magnetic flux was contained within the machine by using a ferromagnetic shield [24].

## E. HTS MOTOR TEST RESULTS

The measured results of the performance testing for the homopolar motor are presented in Table 5.1.

| Armature Current (A) | Field Winding Current (A) | Field Winding Temp (K) | HTS Conductor Electric Field (Uv/cm) | HTS Field Winding Power Loss (W) | DC Motor Speed (RPM) | DC Electrical Power In (hp) | Dc Motor Power Out (hp) |
|---|---|---|---|---|---|---|---|
| 30,000 | 100 | 4.2 | 0.1 | 0.7 | 11,700 | 160 | 143 |
| 30,000 | 120 | 4.2 | 1.0 | 8.4 | 11,700 | 181 | 167 |
| 30,000 | 70 | 28 | 0.1 | 0.5 | 11,700 | 142 | 122 |

Table 5.1. NSWC homopolar motor measured performance test results (From Ref. 24.)

### 1. Power Output

The power output for various field currents in Table 5.1 is given in horsepower. The conversion from horsepower to Watts is given by:

$$P[W] = P_{hp} \times 745.6 \tag{5-2}$$

where $P_w$ is the power in Watts, $P_{hp}$ is the power in horsepower, and 745.6 is a conversion factor. Using the input and output power to calculate efficiency revealed an efficiency decrease of 26% when the field winding was operated at 28 K instead of 4.2 K. The motor was most efficient operating with the field winding at 4.2 K and a field current of 120 A. This demonstrates the effect that the operating temperature has on the motor's performance.

## F. STATUS OF HTS MOTOR DEVELOPMENT

Work is ongoing to develop a Homopolar motor for shipboard propulsion applications. The high current carrying brushes are the limiting technology at this time. An effective power conversion system to produce the high current, low voltage DC required for the motor is also required [24]. General Atomics Corporation (GA) has built a 500 kW Test Stand Motor and a 3.7 MW motor funded by ONR [24]. LTS NbTi coils were used, but the design allows for a direct transition to HTS coils whenever it becomes cost effective and practical to do so [24].

## G. COMPARISON OF THE GA MOTOR TO OTHER TECHNOLOGIES

### 1. GA Baseline Motor

For comparison purposes, the GA baseline homopolar motor has been scaled to the reported operating points for several selected motors that have been built recently [24]. Table 5.2 provides the details of the comparison.

| | MW | rpm | Length, [m] | Diameter, [m] | Wt, [tons] |
|---|---|---|---|---|---|
| AMSC 5000 HP | 3.7 | 1800 | 1.59 | 1.12 | 6.81 |
| Homopolar | 3.7 | 1800 | 1.36 | 1.00 | 4.4 |
| PMM DERA | 2.45 | 308 | 1.55 | 1.5×1.48 | 13 |
| Homopolar | 2.45 | 308 | 1.91 | 1.40 | 12 |
| PMM DARPA | 1.5 | 1800 | 1.04 | 0.74×0.74 | 1.69 |
| Homopolar | 1.5 | 1800 | 1.19 | 0.80 | 2.2 |
| AC Ind IPS | 19 | 150 | 4.35 | 4.0×4.5 | 117.4 |
| Homopolar | 19 | 150 | 3.81 | 2.80 | 95.9 |

Table 5.2. Baseline homopolar motor design scaled for comparison to selected motors (After Ref. 24.)

The first row in Table 5.2 corresponds to an HTS synchronous motor produced by American Superconductor. The third row is a PMM developed in the U.K. [24]. The fifth row is a PMM motor developed for DARPA, and the seventh row is the 19 MW IPS motor [24]. As the table shows, the homopolar motor has a smaller size and weight compared to all motors with the exception of the DARPA motor.

### 2. GA Advanced Motor

The GA baseline motor design was primarily oriented toward technology validation for the brushes and superconducting coils and is not the most compact configuration for a homopolar machine [24]. Estimates for an advanced motor are provided in Table 5.3 and compared to those of Table 5.2. The estimates take into account improvements such as: three superconducting coils instead of two, operation at a higher field level, and two rotors on the same shaft [24].

| | MW | rpm | Length, [m] | Diameter, [m] | Wt, [tons] |
|---|---|---|---|---|---|
| AMSC 5000 HP | 3.7 | 1800 | 1.59 | 1.12 | 6.81 |
| Homopolar | 3.7 | 1800 | 1.5 | 0.74 | 2.80 |
| PMM DERA | 2.45 | 308 | 1.55 | 1.5×1.48 | 13 |
| Homopolar | 2.45 | 308 | 2.10 | 1.03 | 7.7 |
| PMM DARPA | 1.5 | 1800 | 1.04 | 0.74×0.74 | 1.69 |
| Homopolar | 1.5 | 1800 | 1.19 | 0.59 | 1.4 |
| AC Ind IPS | 19 | 150 | 4.35 | 4.0×4.5 | 117.4 |
| Homopolar | 19 | 150 | 4.2 | 2.06 | 61.2 |

Table 5.3. Advanced homopolar motor design scaled for comparison to selected motors (After Ref. 24.)

Table 5.3 indicates that the improved homopolar motor is smaller and weighs less than all of the other motors. The average weight reduction considering all of the motors in Table 5.3 is 14.53 tons. The reduced size and weight are important factors to consider for a shipboard propulsion system.

### 3. IPS Advanced Induction Motor

#### *a. Weight Comparison*

Table 5.4 provides a comparison of an advanced homopolar motor with the 19 MW IPS motor [24]. The motor along with its associated filter, converter, or rectifier is compared. The table shows that the homopolar system is about fifty-six tons lighter than the induction motor system.

| | AC Induction [tons] | Homopolar [tons] |
|---|---|---|
| Generator | 50.5 | 51.5 |
| Converter | 9.0 | NA |
| Filter | 4.3 | NA |
| Rectifier | NA | 0.85 |
| Buck Converter | NA | 4.1 |
| Motor | 117.4 | 63.2 |
| Total | 181.2 | 120 + 5 (bus) |

Table 5.4. 19 MW, 150-RPM advanced homopolar system weight comparison with AC induction motor system (After Ref. 24.)

### *b. Volume Comparison*

The homopolar system consumes a smaller amount of ship volume than the AIM Drive. Table 5.5 provides a comparison of the volume occupied by the induction motor system and the homopolar motor system. As the table shows, there is a volume savings of approximately 43 cubic meters with the Homopolar system.

| | **AC Induction [$m^3$]** | **Homopolar [$m^3$]** |
|---|---|---|
| Generator | 34.7 | 38 |
| Converter | 21.0 | NA |
| Filter | 10.6 | NA |
| Rectifier | NA | 2.8 |
| Buck Converter | NA | 12 |
| Motor | 44.7 | 15.0 |
| Total | 111 | 67.8 |

Table 5.5. 19 MW, 150-RPM advanced homopolar system volume comparison with AC induction motor system (After Ref. 24.)

## H. CHAPTER V CONCLUSION

This chapter has introduced the SDCHM and has discussed it properties and advantages. The SDCHM tested by the Navy was described and its test results were discussed. The motor that is being developed by General Atomics was also presented and compared to other motor technologies. The results presented in this chapter indicate that a significant size, weight, and volume reduction can be realized in a ship propulsion drive through the use of a DC homopolar system. Although significant advances have been made in the development of brushes and coolers for these systems, the two are still the main obstacle preventing the employment of this system in a shipboard electric drive. The converter for this type of system also needs to be addressed before a homopolar motor can be employed for propulsion purposes. Converters are discussed in the next chapter.

# VI. POWER CONVERTERS FOR CONTROLLING PROPULSION MOTORS

## A. INTRODUCTION

The electric motors discussed in the previous chapters all require power conversion and control equipment to provide effective speed control for the motor. In many cases, power converters are driving motor technology. The motors discussed in the previous chapters are not very beneficial without an appropriate controller or converter. The controllers must be engineered to accurately control the motor's speed while introducing a minimal amount of harmonics. This chapter will present the various converters that are used to control large propulsion motors.

## B. REQUIREMENTS

The number of motor phases, the phase connections, and the rated machine frequency drive the topological options for the propulsion converter [3]. These options are further constrained by available semiconductor device capabilities: low-voltage, lower-power, fast-switching devices or high-voltage, slow switching devices [3]. Converters for naval propulsion applications need to be engineered to withstand a single component failure and still function at reduced capacity [3]. Converters need to be simple, reliable, and rugged but they need to include circuitry to provide the best waveform fidelity for acoustic performance [3]. The units must permit convenient monitoring for diagnostics and troubleshooting, minimize source and load harmonics, be immune to problems with Electromagnetic Interference (EMI), and cooling, be modular to expedite maintenance and repair, and minimize cost [3].

## C. POWER DEVICE TECHNOLOGY

Technological advances in power electronics devices are a major factor in power converter technology. The requirements for high-power semiconductor devices include high blocking voltages, low leakage currents, and high switching frequencies with low conduction drops and losses [3]. The technology for these devices is changing fairly rapidly. The current ratings for power switching devices can be found by examining their respective data sheets.

## D. AC POWER CONVERTERS

This section will discuss the various medium-voltage propulsion converter options for the Navy's electric ship.

### 1. Cycloconverter (CC)

Direct frequency changers are known as cycloconverters. They convert an AC supply of utility frequency to a variable frequency [14]. The cycloconverter provides an output frequency that ranges from 0–0.5 $f_s$, where $f_s$ is the supply frequency [14]. For better waveform control and to reduce harmonics, the output frequency is usually limited to 0.33 $f_s$ [14]. This small range of frequency variation is suitable for low-speed, high-power applications such as that found in a ship drive. Cycloconverters are currently used in many large vessels such as icebreakers and cruise liners. Due to their large size as compared to other converters, cycloconverters are not appropriate for use in a small warship where space is at a premium. Other limitations include its limited output frequency range, its low power factor, the complex spectra of input and output harmonics that require passive filtering, and the large number of power devices to control [3].

### 2. Synchroconverter

Synchroconverters are indirect frequency converters that consist of a rectification (AC-DC) and an inversion (DC-AC) stage. A large link inductor separates the rectifier and inverter stage. The synchroconverter is also known as a Line Commutated Inverter (LCI) or a Current-Source Inverter (CSI). This type of converter is used extensively in the cruise liner industry [3]. The inverter section is made up of thyristor devices that are naturally commutated by the machine back EMF [3]. In order to be naturally commutated, the machine must operate at a leading power factor [3]. At low speed, where the back EMF is low, the converter control is required to be more complex to ensure thyristor commutation [3]. The large link inductor creates a DC current that is routed through the respective thyristors and machine phases, creating quasi-rectangular phase currents [3]. There are substantial harmonics in the phase currents that lead to drive derating, torque harmonics, poor input current quality and $dv/dt$ [3]. High values of $dv/dt$ (voltage spikes) can cause power devices such as thyristors to be re-triggered during their recov-

ery period. The re-triggering can damage the thyristor, so the $dv/dt$ needs to be minimized. The output frequency of a cycloconverter is limited by the switching frequency of the Silicon Controlled Rectifiers (SCR) [3]. The advantages of this type of converter are that it has the fewest number of components and it can be connected in series with other cycloconverters to provide redundancy [3]. The main disadvantage is the substantial harmonics on the output waveform [3]. These harmonics make this type of converter unacceptable for a surface combatant [3].

### 3. Pulse-Frequency Modulation (PFM)

PFM is a direct AC-AC frequency conversion strategy, which has been studied by the U.K. Royal Navy [3]. The PFM operates by taking discrete energy packets from the input, storing the energy in a capacitor, and then controlling the release of the energy to give the proper frequency at the output [3]. Since thyristors have a very large power rating, the need for paralleling or multi-level topologies can be eliminated [3]. Thyristor units must be interleaved to achieve waveform fidelity because of the limited switching frequency of the thyristors [3]. Some of the advantages of this type of converter include a low $dv/dt$, and a very high efficiency due to the natural soft-switching operation [3]. These units also have a very high power density. Estimates predict that a 25 MW power converter can achieve a power density of 5.5 MW/m$^3$ with near unity power factor [3].

### 4. Pulse Width Modulation (PWM)

The PWM converter is also an indirect frequency converter. These converters also consist of a rectifier and inverter stage. Instead of having a link inductor like the previous converter, the PWM has a DC link capacitor to provide constant control voltage. At high power, PWM-based converters are typically built using GTOs, GCTs, IGBTs, or HVIGBTs [3]. The configurations may be loosely classified as H-bridge, conventional or multi-level [3]. Conventional configurations can be further classified as hard-switched or soft-switched [3]. PWM converters usually provide stair-stepped phase voltages with high frequency notches and fairly sinusoidal phase currents with smooth motor torque [3]. Current technologies facilitate converters with power densities on the order of 750 kW/m$^3$ with innovations in the area promising to increase that to 2.0 MW/m$^3$ [3].

## E. CHAPTER VI CONCLUSION

This chapter has presented a basic review of the power converters available for ship propulsion applications. Their properties, advantages and disadvantages were discussed. Advances in power switching devices are driving converter technology. The converters along with the propulsion motors that were discussed in the previous chapters are being investigated for use in Podded Propulsors (Pods) on surface ships. Pods will be discussed in Chapter VII.

# VII. PODDED PROPULSION

## A. INTRODUCTION

Podded propulsors (Pods) are yielding significant benefits to the commercial shipping industry [19]. These units can also be found on many of the pleasure cruise liners. Ship builders began using pods during the late 1980's and their use has grown ever since. The Alstom/Kamewa pod system known as Mermaid® is currently leading the industry with many of these units already installed in cruise ships. This chapter will discuss the potential benefits of employing pods on surface combatants. Additionally, the different types of pods will be discussed and compared.

## B. TYPES OF PROPULSORS

### 1. Azimuthing Thruster

The idea of having a propulsion arrangement without the use of a shaft originated with the use of the Azimuthing Thruster (AT). The AT is a propulsion configuration in which the prime mover (in this case an electric motor) is connected to the propeller through one or two right angle gears designated as L or Z drives respectively [27]. These types of propulsors are widely employed in the commercial shipping industry. The U.S. Navy's propulsion requirements are obviously significantly different from the commercial sector because of concerns involving noise, vibration, robustness, and survivability. The U.S. Navy is not actively pursuing the use of the AT for ship propulsion because of the additional noise and vibration caused by the L or Z gears used in the AT.

### 2. Podded Propulsors

Pods are distinguished from the original thruster in that the prime mover is an electric motor situated in the hub underneath the strut, directly driving the propeller [27]. Pods offer improved efficiency and maneuverability over shafted propulsion systems. The Navy is currently researching the use of pods on future surface combatants. Although the pods have been proven in large commercial ships, their effectiveness, robustness, and reliability have yet to be proven in a warship.

## C. BENEFITS OF USING PODS

Some of the benefits of using pods include increased efficiency and maneuverability, and increased design flexibility [28]. Pods increase maneuverability by being able to rotate through 360° to provide thrust in any direction needed. Eliminating the long shaft line associated with a conventional drive increases design flexibility. By applying hydrodynamic pod and hull design improvements, fuel consumption can be reduced and propulsion efficiency can be increased [29]. Pods also simplify the shipbuilding process. Complete podded propulsion systems can be delivered and fitted in days, thus avoiding the lengthy installation of a traditional system [29]. Using pods can eliminate much of the auxiliary and support equipment associated with a traditional propulsion system. For example, in a podded system, the rudder, steering gear, propeller, propulsion motor, main propulsion shaft, the shaft bearings, the thrust bearing, and the shaft seals are all integrated into a single unit [29]. Figure 7.1 compares a podded drive with a conventional drive. The pod in the upper half of Figure 7.1 contains all of the components of the conventional shaft line that is shown in the lower half of Figure 7.1. Figure 7.2 provides a detailed view of a typical pod. A commercial vessel is shown in Figure 7.3 with two pods mounted under the aft portion of the vessel in the pulling configuration.

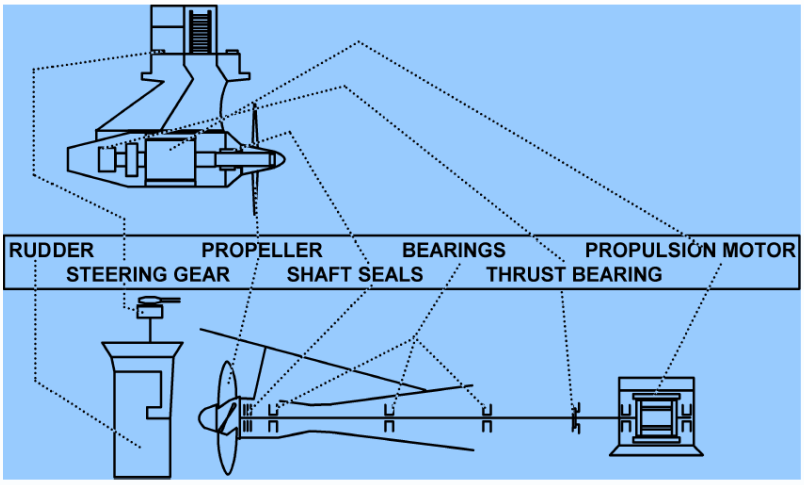


Figure 7.1. Demonstration of integrated architecture of pods versus conventional propulsion systems (From Ref. 30.)

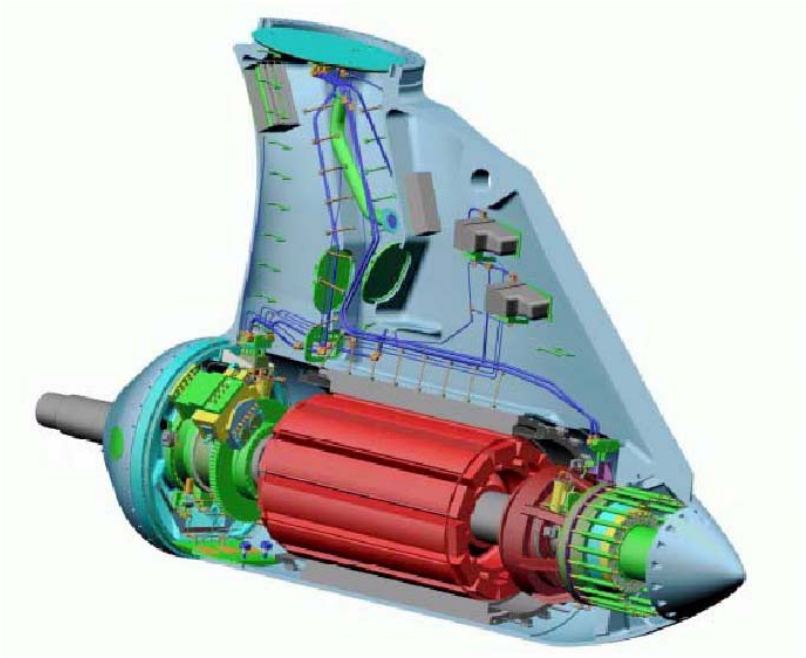

Figure 7.2. Typical design of a podded propulsor (From Ref. 30.)


Figure 7.3. Picture showing the mounting of two pulling type pods (From Ref. 30.)

## D. MOTOR TYPES BEING USED

Pods used in commercial shipping can employ field wound synchronous motors or induction motors. Pods designed for a warship would need to use a motor that is much smaller and more power dense, such as a PMSM. Permanent magnet propulsion motors are being developed by several commercial firms to fulfill the requirement for more power dense motors to be used in pods. HTS synchronous motors and the SDCHM are being researched and developed for potential employment in pods.

## E. EFFICIENCY BEFEFITS OF PODS

Pods can be either the pulling or the pushing type, which means that the propeller can be mounted at the forward or the aft end of the unit [29]. Pulling type pods have a much better efficiency than the pushing type [29]. This is due to the fact that the wake field through the propeller is not disturbed by a hub or shaft [28]. Pushing pods are hydro dynamically similar to a normal propeller arrangement [29]. Unlike a conventional system, where the propeller axis has to be more or less parallel to the bottom line of the ship, podded propulsor shafts can be oriented in any direction [29]. This ability allows the pod shaft to be oriented parallel to the flow of water along the aft hull of the ship thereby achieving a better correlation with the wake field [29]. Using pods can increase efficiency by as much as 10-15 %. The increase in efficiency reduces fuel consumption [29].

## F. CHAPTER VII CONCLUSION

This chapter has introduced pods and has discussed their potential benefits. The two main types of podded propulsors were discussed and they included the Azimuthing Thruster (AT) and the direct-drive podded propulsor. The benefits of using direct-drive pods include increased maneuverability, better design flexibility, and improved efficiency. This technology is very mature in the commercial industry, but has yet to be proven in a warship application.

The U.S. Navy successfully demonstrated the feasibility of applying the technology discussed in this thesis to a naval warship. The Navy's IPS program proved that the electric ship concept was a very attainable goal. The IPS program is the focus of the next chapter.

# VIII. U.S. NAVY IPS PROGRAM

## A. INTRODUCTION

The majority of this study has discussed the various motors being considered for use in an electric ship drive. This chapter will discuss the final test results of the Navy's Full Scale Advanced Development (FSAD) program which demonstrated the Navy's IPS [31]. The system was used to test the IPS in a simulated shipboard environment. Figure 8.1 shows a block diagram of the IPS and its major components. The figure shows the Propulsion Motor Module (PMM) consisting of the propulsion motor and its associated controller, the Power Generation Modules (PGM), Power Distribution Modules (PDM), Power Conversion Modules (PCM), and the load banks. Also shown are the AC and DC voltage busses.

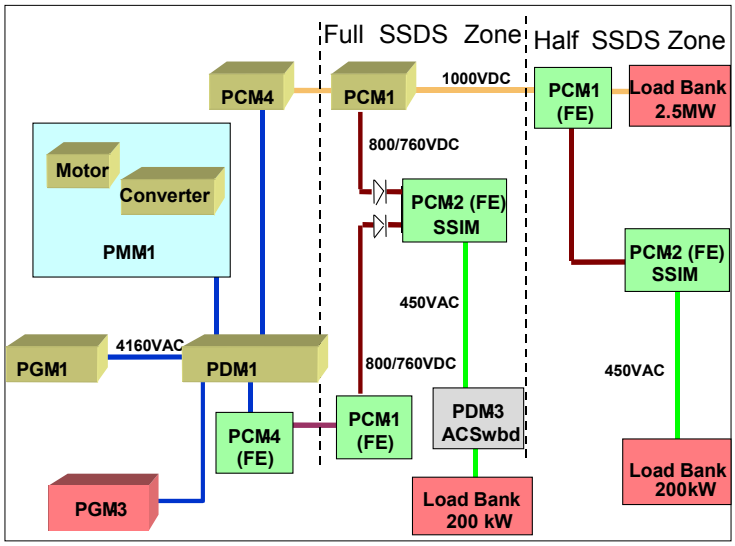


Figure 8.1. Diagram of FSAD Land Based Test Site (From Ref. 31.)

## B. PROPULSION MOTOR MODULE

### 1. Propulsion Motor

#### *a. Characteristics*

Electric propulsion in the IPS was provided from a 19 MW - 150-rpm, 15-phase Propulsion Motor Module (PMM-1) designed and manufactured by Alstom Corpo-

ration. The module consisted of a propulsion converter, harmonic filter and Advanced Induction Motor (AIM) [31]. The 15 phases in the motor allow for fine speed control, which simulates a synchronous motor's flexibility [32]. They also provided the best noise performance and minimal stator design impact [31]. An even number of phases was avoided to preclude harmonic torque pulsations from exciting mechanical resonances within the machine [32]. Slip was kept to a minimal 1.23% at rated conditions and the motor's efficiency was 95.7% [32]. The propulsion shaft line was connected to a 25,000 hp Froude waterbrake to emulate a propeller load [31].

#### *b. Advantages*

An induction motor was preferred over a synchronous motor due to the added complexity, cost, weight and size of a synchronous motor [32]. Some of the other advantages of the induction motor over the synchronous motor are a simpler, rugged, and reliable rotor design, no insulated rotor components and no added control complexity, losses or maintenance related to an exciter [32]. To improve shock and vibration performance, additional and thicker stator ribs, heavier end plates and end frame bearings were added to develop a stiffer stator structure [32]. Stronger metal alloy was used in the rotor construction and the air gap was doubled to prevent the rotor from contacting the stator during shock deflections [32]. The additional design measures added to the machine's ability to resist noise transmissions [32]. The fifteen-phase design was selected to achieve stator and rotor slot/phase/pole ratios of 1-to-1 to meet the very stringent acoustic requirements for a naval combatant ship [32].

### 2. Propulsion Converter

#### *a. Characteristics*

The propulsion converter was an H-bridge type converter that consisted of a 3 phase, 6 pulse thyristor controlled rectifier and a 15 phase Pulse Width Modulated (PWM) Voltage Source Inverter (VSI) with an output of 0–3700 $V_{RMS}$ and 0–15 Hz [31]. Since harmonic frequencies can cause overheating in the rotor of a supply generator, the PWM included a harmonic filter to protect the generator rotor from overheating from the substantial $5^{th}$ harmonic frequency [31]. Figure 8.2 shows a schematic diagram of the PWM converter. Shown in the figure are 15 H-bridges, one for each phase.

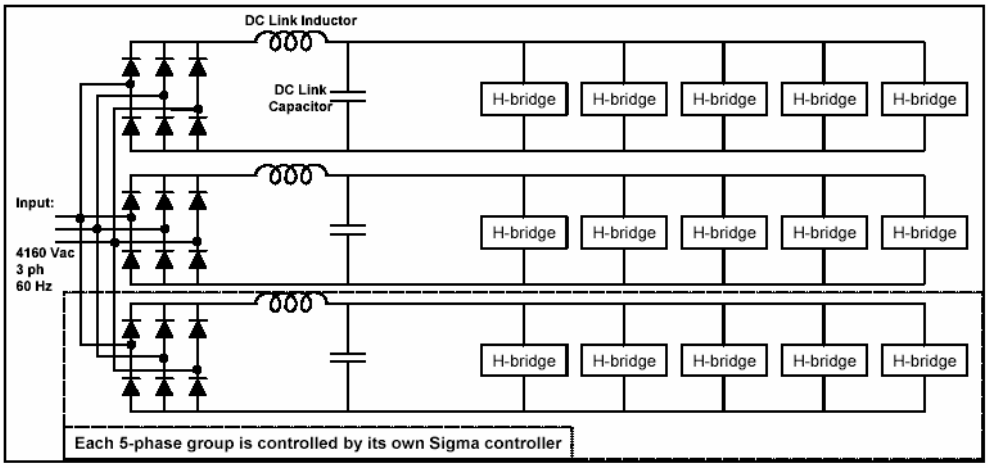

Figure 8.2. IPS PWM converter schematic (From Ref. 32.)

### *b. Advantages*

A PWM converter was selected over a load commutated inverter (LCI) or cycloconverter for numerous reasons [32]. Since a PWM converter does not require a synchronous motor to maintain a controlled load commutation, the advantages of an induction motor became available with the PWM drive [32]. The PWM converter provided the ability to selectively control the output waveform for a more sinusoidal shape [32]. Selective shaping of the output reduced harmonics resulting in lower motor noise than was possible with other converters [32]. Other advantages of PWM converters over LCI and cycloconverters are a higher, more constant power factor for better efficiency, constant harmonic frequencies to ease any supply filtering required and smaller size and weight [32]. The FSAD unit was only 2.0x4.0x2.5 m and weighed approximately 17,000 kg, significantly smaller than commercial units of any power topology [32]. Table 8.1 compares the IPS design with standard commercial drive technologies. The table compares the IPS with a rectifier and a synchroconverter being used in the U.K. Also listed for comparison is the cycloconverter currently being used on the U.S. Coast Guard Icebreaker *Healey*.

| Converter (Type) | Rating | Volume [$m^3$] | Weight [tons] |
|---|---|---|---|
| IPS (PWM) | 19 | 905 | 1.12 |
| UK Type 23 | 1.5 | 191 | 0.28 |
| USCG Healey | 11.2 | 455 | 1.24 |
| UK Oiler | 7.0 | 277 | 0.741 |

Table 8.1. Comparisons of Converter Technologies (After Ref. 33.)

## C. IPS SYSTEM COMPONENTS

All of the IPS equipment in the FSAD model was provided a designation to reflect the modular architecture of the IPS concept [31]. The modular architecture incorporated an Integrated Fight Through Power (IFTP) capability in the SSDS [31]. The IFTP concept provided for fully automatic fault clearing, reconfiguration of power and management of generated power, and stored energy sources to isolate the fault to damaged zones [31]. This provided uninterrupted power to undamaged areas. Other components that made up the IPS included Power Generation Modules (PGM), Power Distribution Modules (PDM), and Power Conversion Modules (PCM). These components will not be discussed in this chapter. Details relating to these components can be found in [31].

## D. IPS PERFORMANCE TESTING RESULTS

The primary objective of the IPS FSAD test plan was to characterize the major power interfaces under steady state and dynamic conditions through the power range of the propulsion motor [31]. The dynamic and steady state results were then compared to design goals. The results provided are worst-case deviations for parameters under the test conditions [31].

### 1. Power Quality

With the exception of harmonic content, the voltage and frequency tolerance at the main AC bus of 4160 VAC was maintained within the design goals as shown in Table 8.2, which were based on commercial industrial power requirements [31]. The harmonic voltage distortion was somewhat greater than originally anticipated because of a change in the control voltage scheme for the DC link of the propulsion converter [31]. The in-

creased harmonic distortion did not develop any issues of compatibility with the main generator due to its inherent design margin, but the design of the SSDS main rectifier was modified to accommodate the higher harmonic distortion level expected [31].

| Parameter | FSAD Design Goals | Test Results |
|---|---|---|
| Voltage Tolerance | ± 10% | + 1.01% |
| Frequency Tolerance | ± 5% | + 3.49% * |
| Voltage THD | < 10% | 15.92% |

** Based on a 3.22 % frequency droop setting*

Table 8.2. 4160 VAC main bus steady state interface design goals (From Ref. 31.)

The power quality interface goals of voltage tolerance and ripple at the main DC bus of 1000 VDC were not fully satisfied as indicated in Table 8.3, but the power quality performance at the ship service voltage of 450 VAC still remained within MIL-STD-1399 requirements as illustrated in Table 8.4. [31].

| Parameter | FSAD Design Goals | Test Results |
|---|---|---|
| Voltage Tolerance | +/- 0.50% | + 0.80% |
| Voltage Ripple | ≤ 1.5% | 3.20% |

Table 8.3. SSDS main rectifier 1000 VDC Bus Steady State Interface Design Goals (From: 31.)

| Parameter | FSAD Design Goals | Test Results |
|---|---|---|
| Voltage Tolerance Line to Line | ± 7% | - 5.09% |
| Line Voltage Unbalanced | 3% | NA |
| Frequency Tolerance | ± 3% | + 0.03% |
| Voltage IHD | 1% | 0.98% |
| Voltage THD | 2% | 1.43% |

Table 8.4. SSDS zone inverter 450 VAC ship service bus steady state interface design goals (From Ref. 31.)

The interface design goals for power quality at the zonal DC bus were met for voltage tolerance and slightly exceeded for voltage ripple as depicted in Table 8.5 [31].

| Parameter | FSAD Design Goals | Test Results |
|---|---|---|
| Voltage Tolerance | + 5%, - 6% | + 0.21% |
| Voltage Ripple | ≤ 1% | 1.12% |

Table 8.5. SSDS DC-DC bus converter nominal 800 VDC (760 VDC) bus steady state interface design goals (From Ref. 31.)

As shown in Table 8.6, the transient performance of voltage and frequency excursions and durations at the main AC bus of 4160 VAC was within the interface design goals [31].

| Parameter | FSAD Design Goals | Test Results * |
|---|---|---|
| Worst Case Voltage Excursion | + 20%, - 15% | + 17.9% |
| Voltage Transient Recovery Time to Return | 1.5 sec max | 1.3 sec |
| Worst Case Frequency Excursion | ± 10% | + 5.1% |
| Frequency Transient Recovery to Steady | 5 sec | 1.3 sec |

** Based on test results from 100% rated propulsion power step unload*

Table 8.6. 4160 VAC main bus dynamic interface design requirements (From Ref. 31.)

### 2. Harmonics Performance

The harmonic characteristics of the IPS FSAD are explained using Individual Harmonic Distortion (IHD), Total Harmonic Distortion (THD), and Total Demand Distortion (TDD) [31]. The term TDD is more meaningful for assessing overall harmonic current content than THD since it is based on a constant value of rated load current rather than a fundamental current that varies according to the load condition [31]. The harmonic content of the 4160 VAC distribution system, as influenced by the propulsion converter, was higher than originally projected as indicated by Figures 8.3-8.6 [31]. The

harmonic filter adequately reduced the higher harmonic content to protect the generator and aided in achieving power quality to user loads [31]. The actual current harmonic performance of the converter was close to that predicted for THD and TDD current as indicated in Figure 8.3. The TDD current was lower than the THD current for lower propulsion power and become essentially the same as propulsion power approached 100 % rated power [31]. The THD current seemed to decrease as propulsion power increased giving a false impression that the level of harmonic current content was decreasing. The actual and predicted THD current maintained a more consistent comparison to each other as compared to the TDD current values due to the normalization with the fundamental current at each particular propulsion power level [31].

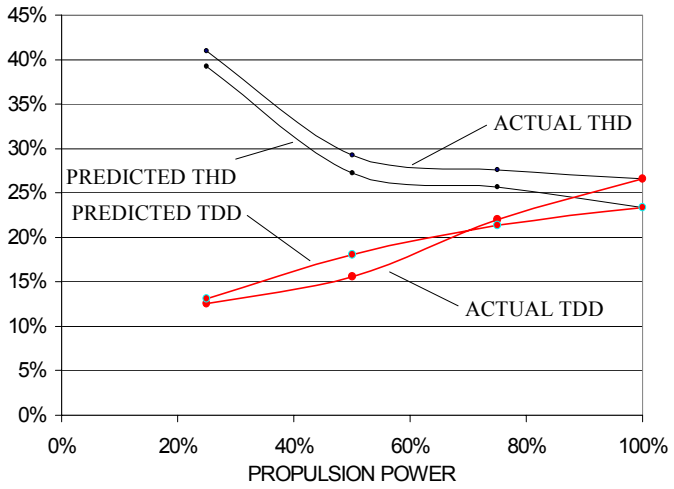


Figure 8.3. Converter current distortion (From Ref. 31.)

The actual harmonic current performance of the filter was close to that predicted as shown in Figure 8.4, except at near rated propulsion power where considerably more harmonics were absorbed than predicted [29]. Note that the TDD and THD current remained essentially the same over the entire propulsion power range because the fundamental current in the filter varied little as propulsion power varied [31].

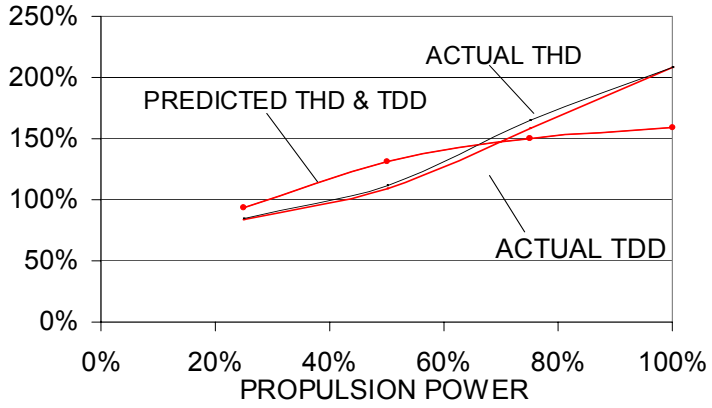


Figure 8.4. Filter current distortion (From Ref. 31.)

As shown in Figure 8.5, the actual current harmonic performance at the generator was better than predicted since the converter was essentially producing the predicted harmonic current content and the filter was absorbing more harmonic current content than predicted [31]. Accordingly, the actual harmonic voltage content at the generator was similar to that predicted as shown in Figure 8.6, except at low and near rated propulsion power [31].

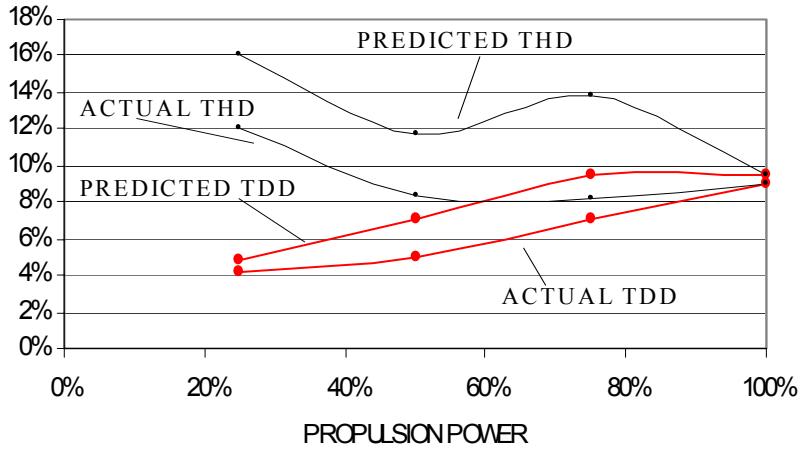


Figure 8.5. Generator current distortion (From Ref. 31.)

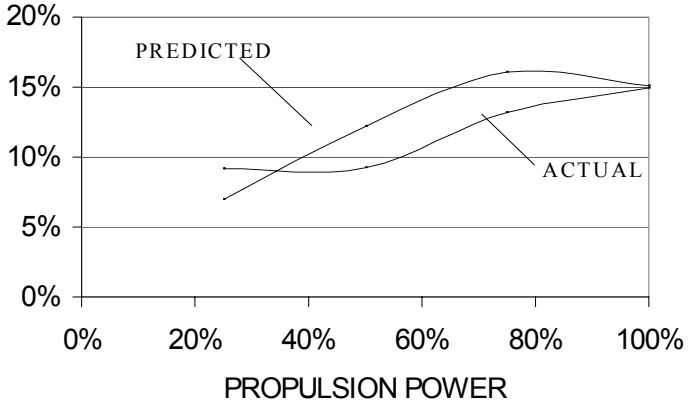


Figure 8.6. Generator voltage distortion (From Ref. 31.)

### 3. Efficiency

Efficiency measurements were recorded during the final test phase and matched predictions as shown in Figure 8.7. Figure 8.8 illustrates the projected efficiencies of the motor and converter individually and overall. Reduced propulsion power operations on 10 phases of the propulsion converter/motor were somewhat more efficient than 15 phases as indicated in Figure 8.9. This was due to fewer losses in the converter with 5 phases off. Reducing these losses had a greater improved efficiency and offset the reduction in efficiency caused by the motor being magnetized with 10 phases versus 15 phases.

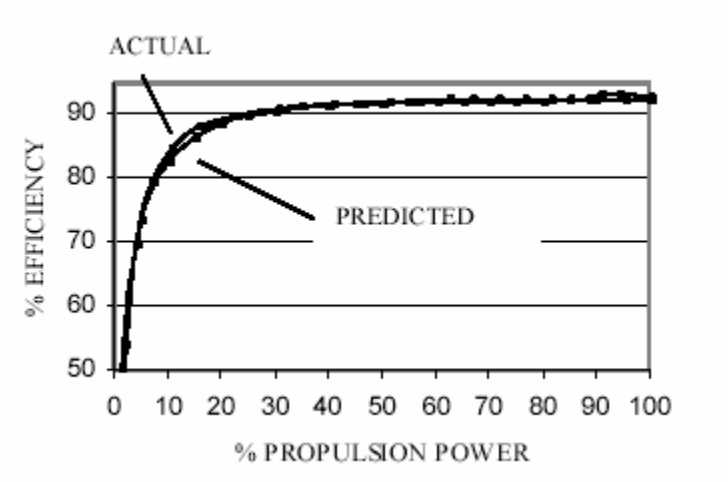


Figure 8.7. Comparison of simulated versus measured propulsion converter/motor efficiency (15-phases) (From Ref. 31.)

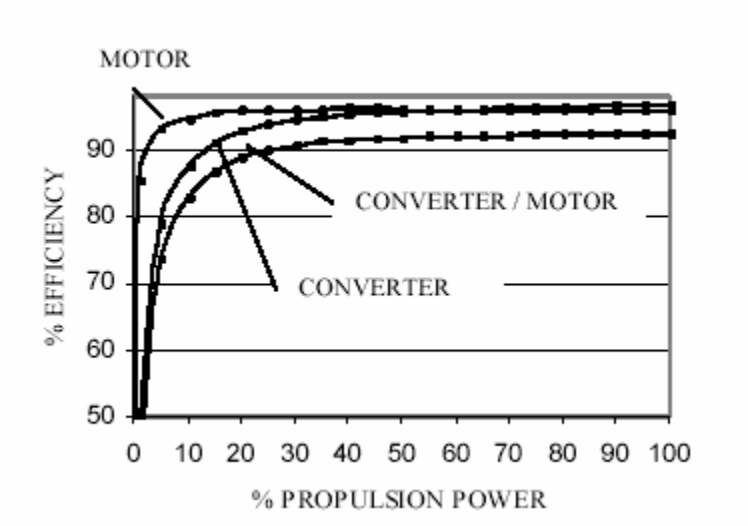


Figure 8.8. Simulated efficiency of propulsion converter, motor, and converter/motor (15-phases)(15-phases) (From Ref. 31.)

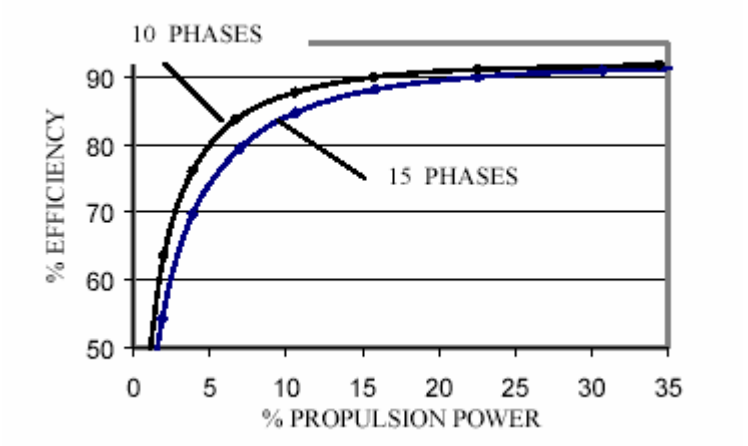


Figure 8.9. Comparison of measured propulsion converter/motor efficiency (10 phases and 15 phases) (From Ref. 31.)

## E. CHAPTER VIII CONCLUSION

This chapter has presented the final IPS test results that pertain to the PMM. The IPS test plan demonstrated the feasibility of employing an IPS in a warship environment. Harmonic performance, efficiency, and the ability to operate at reduced capacity were examined.

The previous chapters did not include a model of a large motor for analysis purposes. Such a model is important to being able to analyze how various changes in the motor's parameters or operating conditions affect its performance. Chapter IX will present the results of modeling a 30 MW induction motor controlled by a voltage source inverter. The associated Matlab m-files are provided in Appendix A.

THIS PAGE INTENTIONALLY LEFT BLANK

# IX. SIMULATION OF A 30 MW INDUCTION MOTOR DRIVE

## A. INTRODUCTION

The purpose of this chapter is to model an electric drive of the size that is likely to be employed on an electric warship. The model assumes a 30-MW induction motor for propulsion power. The control scheme presented will be a voltage source inverter, which employs constant volts/Hertz control. Modeling results of a 20 horsepower (15-kW) motor using volts/Hertz control from Reference 32 will be compared with the results from the 30-MW motor simulations. The comparison is made in order to determine the effectiveness of this type of control method on a very large motor. The model provided here is largely based on a model that was found in Reference 32. The model can be further developed in a later study to demonstrate more advanced control strategies such as PWM control.

### 1. Voltage Source Inverter Driven Induction Motor

Voltage source inverter driven induction motor drives are controlled by changing the 3-phase input voltages into gating signals for power devices in the converter such as SCRs. The frequency and duration of these signals are controlled in order to control the switching of the power devices. The volts/Hertz method keeps the voltage-to-frequency ratio constant in order to control the motor. This helps to maintain a constant air gap flux, which is desirable under changing speed and load conditions.

### 2. Model Development

#### *a. Inverter Waveforms*

The voltage waveforms are presented here along with their respective phases in order to demonstrate the volts/Hertz strategy. The line voltages in terms of phase voltages in a three-phase system with phase sequence abc are [11]:

$$V_{ab} = V_{as} - V_{bs}, \tag{9-1}$$

$$V_{bc} = V_{bs} - V_{s}, \tag{9-2}$$

and

$$V_{ca} = V_{cs} - V_{as}, \tag{9-3}$$

where $V_{ab}$, $V_{bc}$, and $V_{ca}$ the line voltages and $V_{as}$, $V_{bs}$, and $V_{cs}$ are the phase voltages [11]. In a balanced 3-phase system, the sum of the phase voltages is zero:

$$V_{as} + V_{bs} + V_{cs} = 0 \tag{9-4}$$

and the difference between line voltages $V_{ab}$ and $V_{ca}$ is [11]:

$$V_{ab} - V_{ca} = 3V_{as}, \tag{9-5}$$

from which the phase *a* voltage is given by

$$V_{as} = \frac{V_{ab} - V_{ca}}{3}. \tag{9-6}$$

Similarly, the *b* and *c* phase voltages are [11]:

$$V_{bs} = \frac{V_{bc} - V_{ab}}{3}, \tag{9-7}$$

and

$$V_{cs} = \frac{V_{ca} - V_{bc}}{3}. \tag{9-8}$$

Figure 9.1 shows the phase voltages that were derived from the line voltages [11]. In the figure, $G_1$–$G_6$ are the gate voltages applied to the power devices. Frequency control is accomplished by controlling the timing of these stepped voltages.

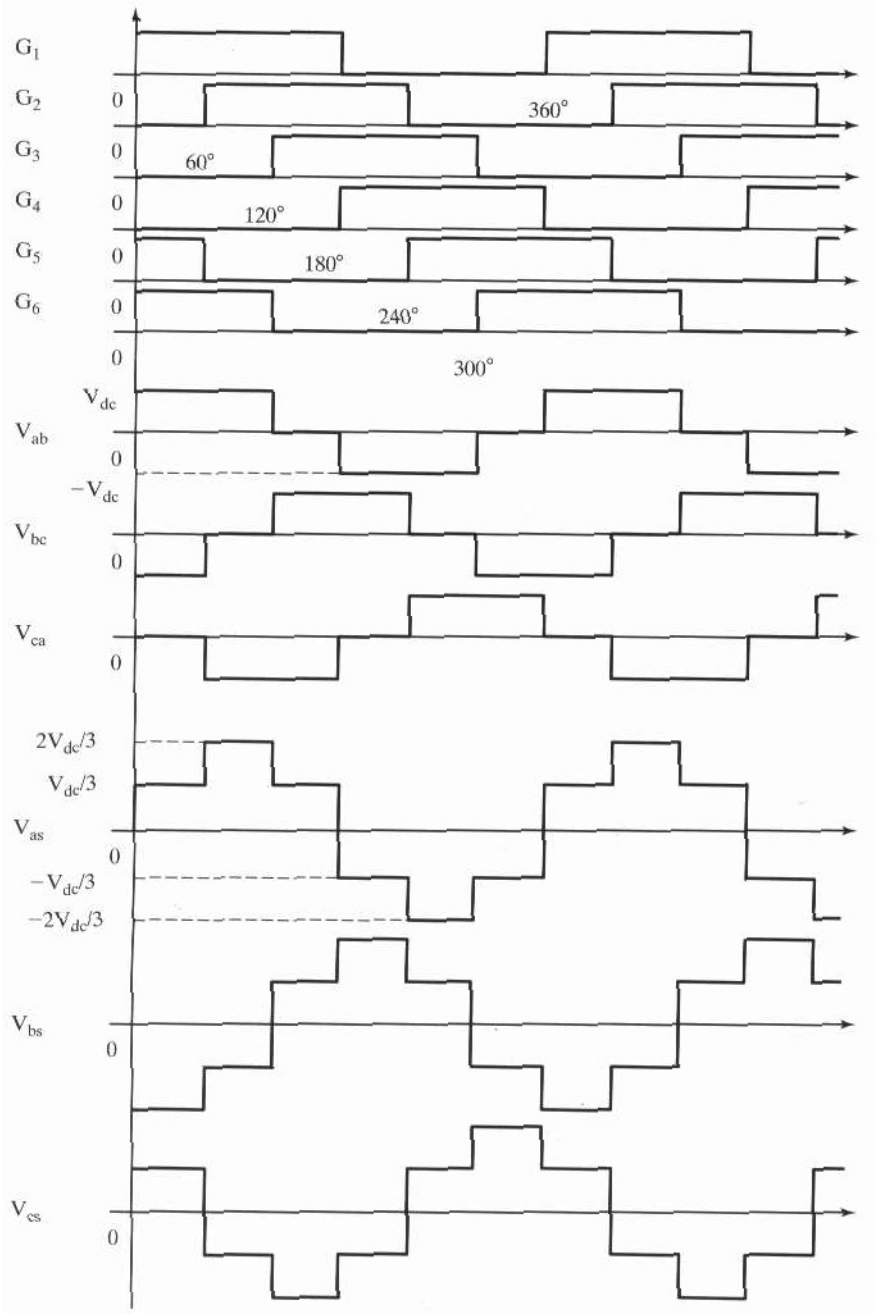


Figure 9.1. Inverter gate (base) signals and line-and phase-voltage waveforms (From Ref. 14.)

### *b. Induction Motor*

The induction motor was modeled in the stationary or stator reference frames using volts/Hertz control. The stator reference frames model has not been derived herein; it is available in References 14 and 32. Figure 9.2 shows the major subsystems of the induction machine model. Moving from left to right in the figure, the per unit speed reference is compared with the motor's actual speed in order to provide the input for the speed controller. The speed controller provides a slip value that is summed with the rotor speed. The slip and rotor speed are multiplied by the base electrical frequency in order to provide the input for the variable frequency source. The variable frequency source provides the volts/Hertz control signals for the motor. Before the control voltages are given to the induction motor, they are converted from the abc reference frames to the qd0 reference frames. From this, the qd0 currents, torque and flux are derived for the machine. The qd0 currents are then converted back to the abc frame for plotting and analysis (the abc and qd0 reference frames are discussed in Reference 14). The Matlab m-files for the motor and model are provided in Appendix A.

Figure 9.3 shows the steady-state operating characteristics of the 30-MW induction motor. Notice the high starting stator current that is present when the motor starts from standstill. Also note that this particular motor has a maximum operating efficiency greater than 95%. As is the case with all induction motors, this motor is most efficient when it is operated at or near its rated speed. Figure 9.4 shows the volts/Hertz control curve for this control method. The curve illustrates the change in voltage required as the frequency is changed. The volts/Hertz ratio has to remain constant for this control method.

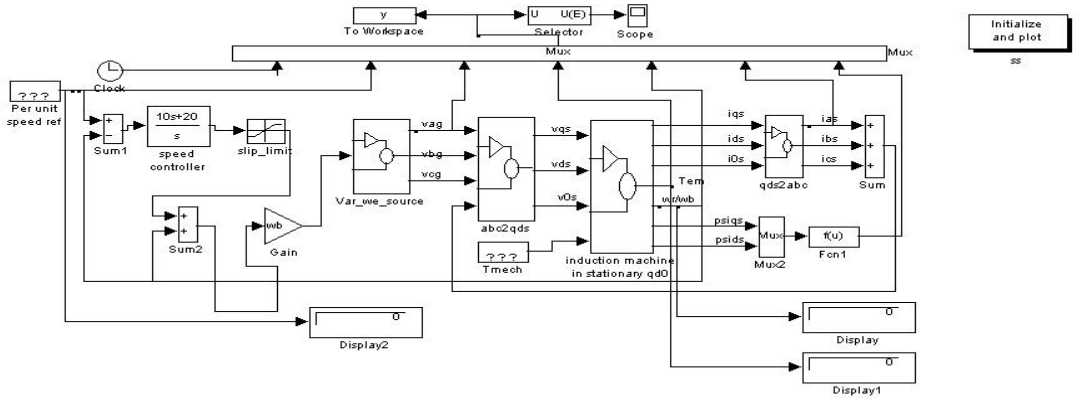


Figure 9.2. Simulink model of a 30-MW induction motor drive (After Ref. 32.)

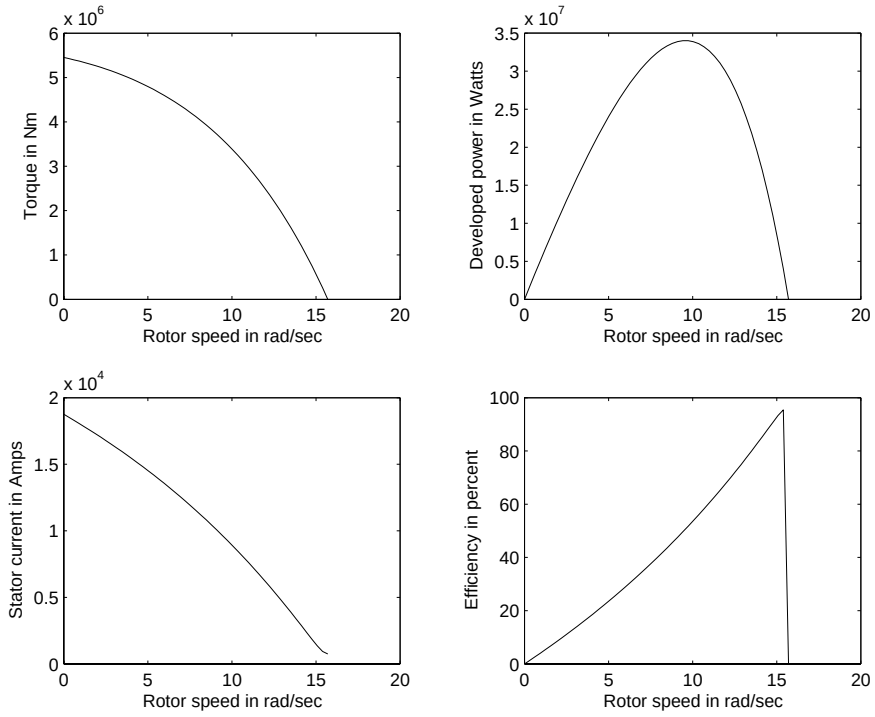


Figure 9.3. Steady-state operating characteristics of the 30-MW induction motor

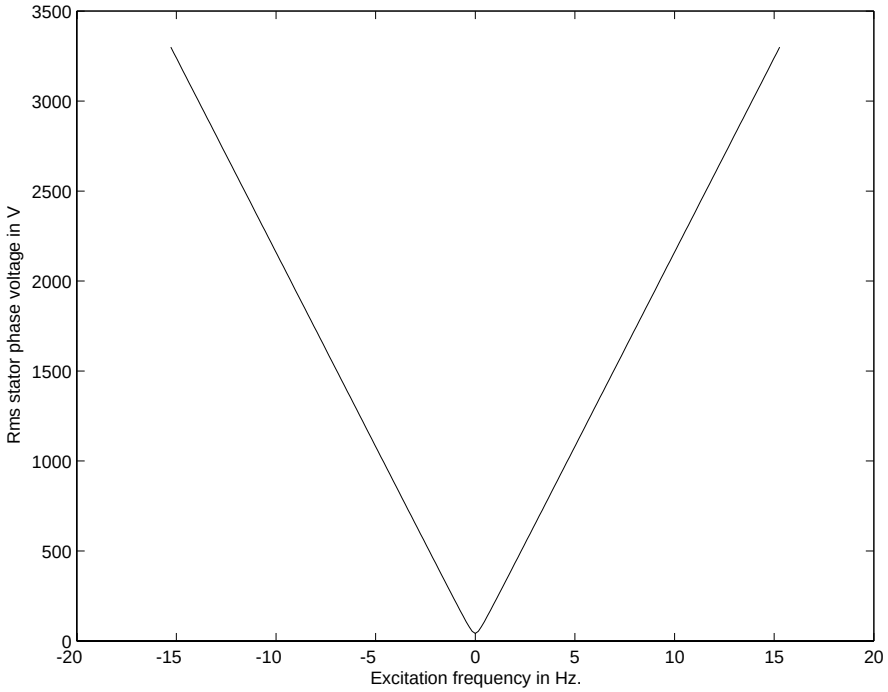


Figure 9.4. Volts/Hertz control curve

### 3. Simulation Results

The simulation consisted of two parts. The first part simulated the motor under changing load conditions. The motor was started from standstill loaded at various times during the simulation timeframe. The second part simulated the motor's response to changing speed commands. The motor was un-loaded for the second part of the simulation. In each case, similar results from a 15-kW motor from Reference 32 were compared to the results from the 30-MW motor. To demonstrate the motor's response to changing load conditions, the motor's drive frequency was held constant while the load torque was changed. Figure 9.5 is a plot of the motor's load versus time. Figure 9.5 shows how the motor's load was changed during the 30-MW motor simulation. A similar load curve was used in the simulation of the 15-kW machine.

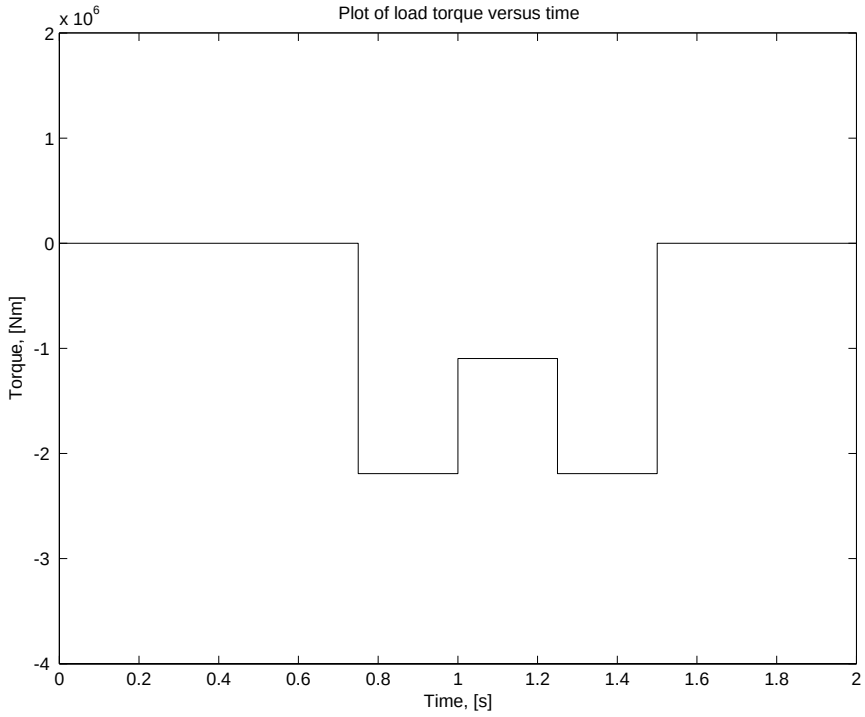


Figure 9.5 Applied motor load during simulation

### *a. 15-KW Motor Control with Changing Load*

For this simulation, the load was first applied at $t = 0.75$ seconds. From $t = 0.75$ seconds to $t = 1.5$ seconds, the load was cycled from zero to $T_{rated}$, from $T_{rated}$ to $0.5 \times T_{rated}$ and from $0.5 \times T_{rated}$ back to zero, where $T_{rated}$ is the motor's rated torque. Figures 9.6 and 9.7 show the simulation results from the 15-kW motor. The first graph in Figure 9.6 is the motor's commanded speed value in per unit. The second graph in Figure 9.6 is the motor's rotational speed in per unit. The motor was able to follow its speed command under the changing load conditions. The third graph in Figure 9.6 shows the phase voltage as the load is changed. The phase voltage remained nearly constant as the load was changed. The phase current, torque, and stator flux are shown in Figure 9.7. The first graph in Figure 9.7 shows the stator phase current. The phase current remained uniform just as the stator voltage did, with the exception of small fluctuations during load changes. The electromagnetic torque is shown in the center graph of Figure 9.7. Load

changes are clearly visible on the torque graph. The third graph in Figure 9.7 shows the stator flux. The flux also remained nearly constant during load changes.

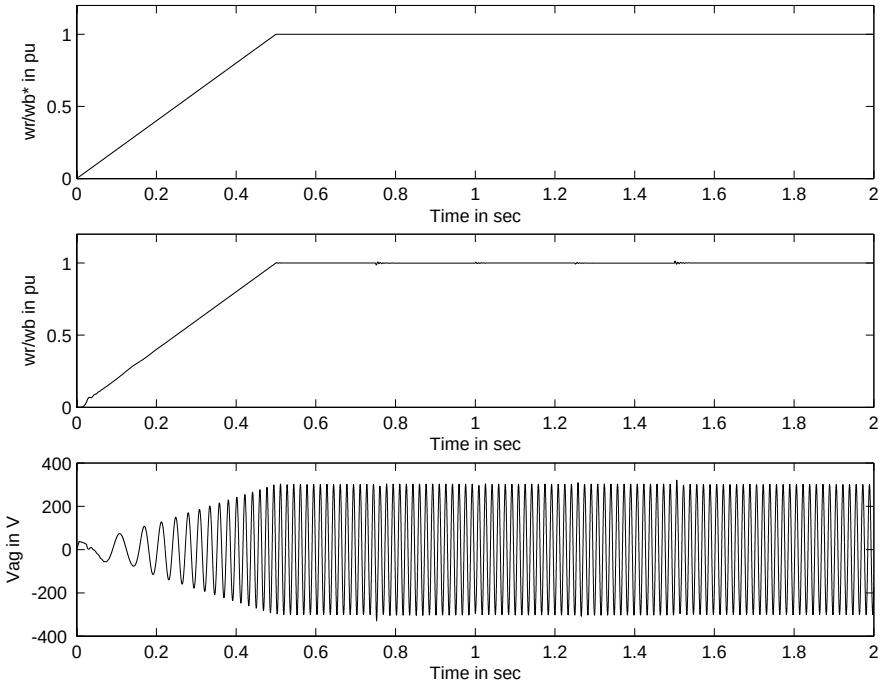


Figure 9.6. 15-kW motor simulation results (From Ref. 32.)

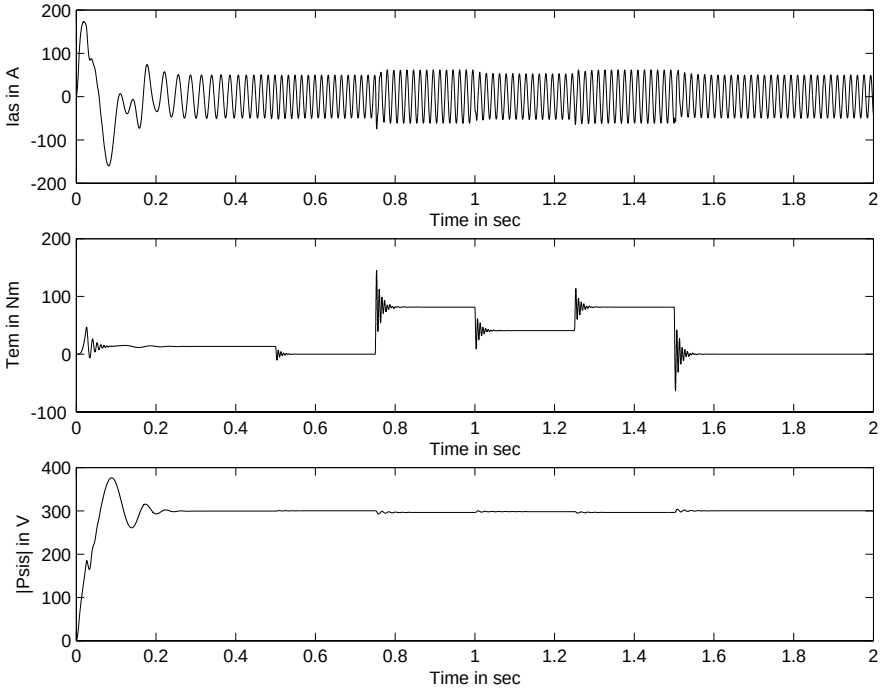


Figure 9.7. 15-kW motor simulation (From Ref. 32.)

### *b. 30-MW Motor Control with Changing Load*

The simulation results from the 30-MW motor simulation under changing load conditions are shown in Figures 9.8 through 9.13. The plots have been placed in separated graph windows in order to provide greater detail. During the description that follows, the graphs from the 15-kW motor simulations from Reference 32 can be referred to for comparison purposes.

Figure 9.8 shows the motor's speed command while Figure 9.9 shows the motor's speed. The fluctuations in Figure 9.9 at $t = 0.75$ and $t = 1.5$ seconds are due to the initial loading and final unloading of the motor, respectively. Except for the fluctuations, this type of control is very effective at maintaining the motor's speed during changing load conditions. Figure 9.10 shows the motor's phase voltage under loaded conditions. Like the 15-kW motor, the phase voltage in the 30-MW motor is uniform except for slight variations during load changes. The phase current is shown in Figure 9.11. It too is nearly uniform during changing load conditions. Figure 9.12 is a plot of the mo-

tor's torque. The torque response to speed changes was not as fast as it was for the 15-kW motor. This was expected since the 30-MW motor is much larger. The flux is shown in Figure 9.13. Notice that it did not remain constant during the simulation. Again, this was expected because of the motor's increased size.

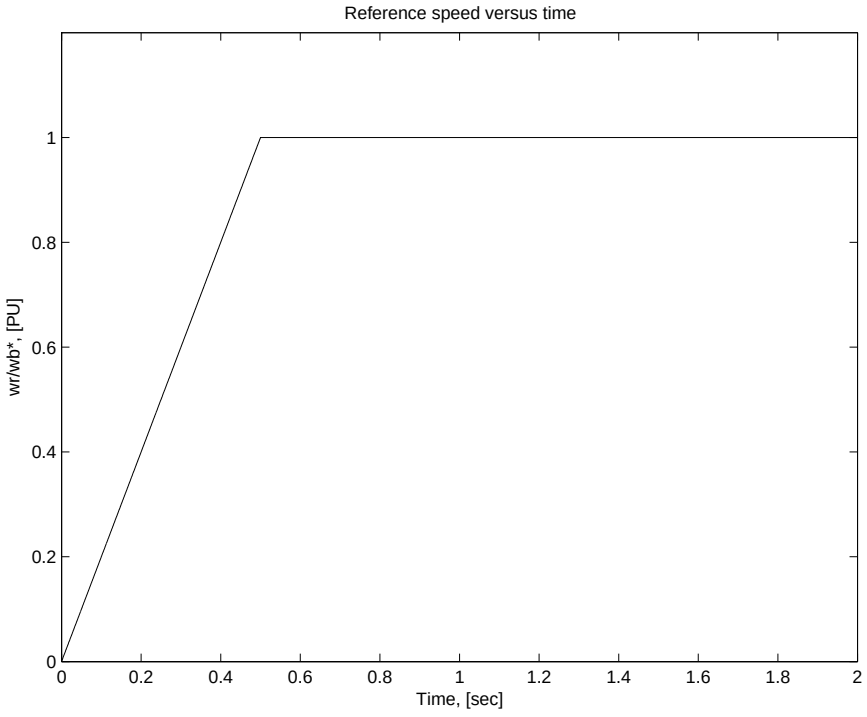


Figure 9.8. 30-MW motor speed command curve

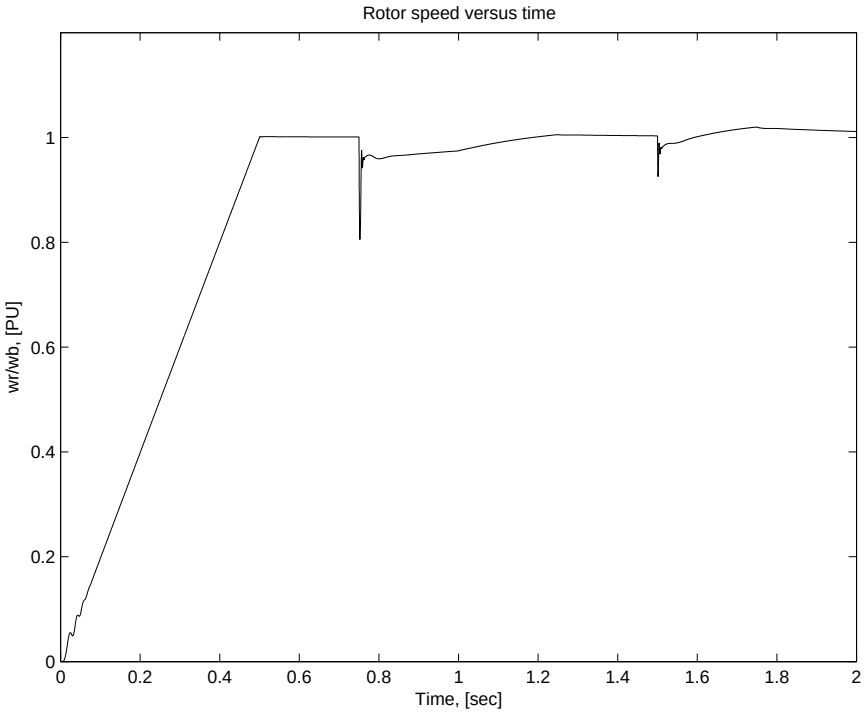


Figure 9.9. 30-MW motor speed response to load changes

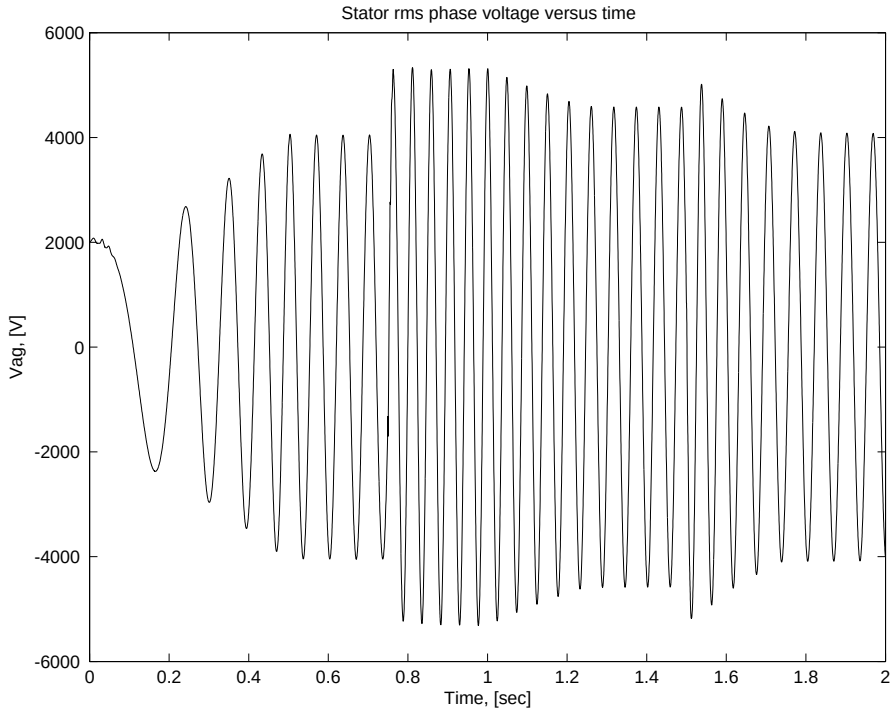


Figure 9.10. Stator RMS phase voltage response to load changes

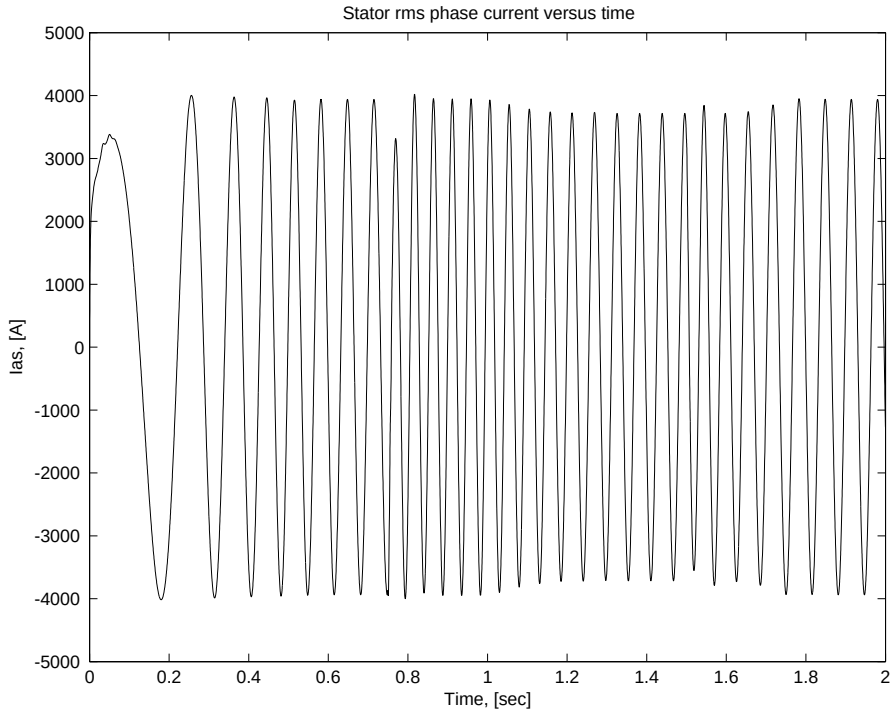


Figure 9.11. Stator RMS phase current response to load changes

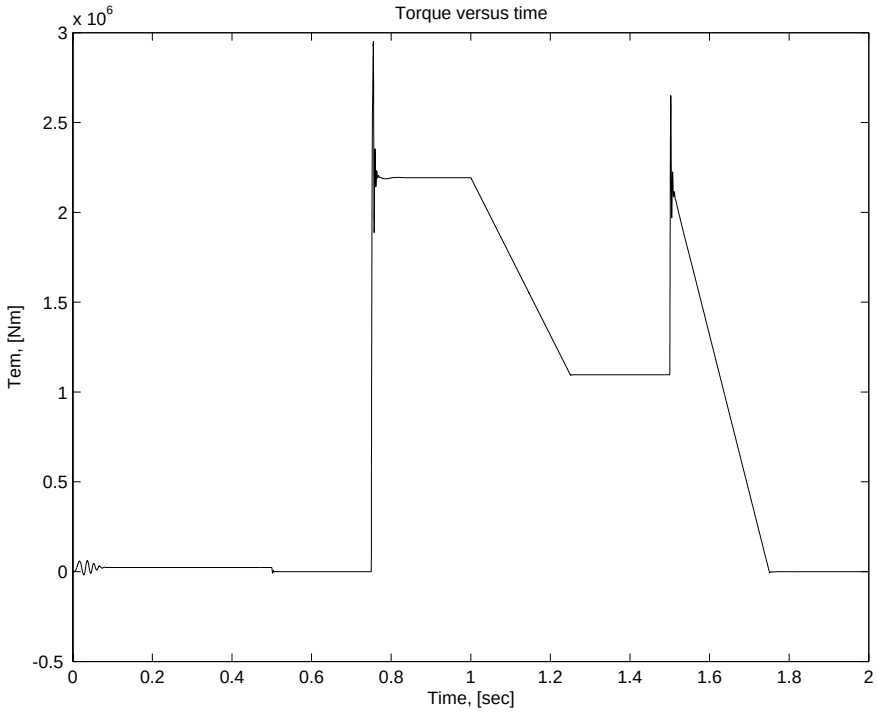


Figure 9.12. Torque response to load changes

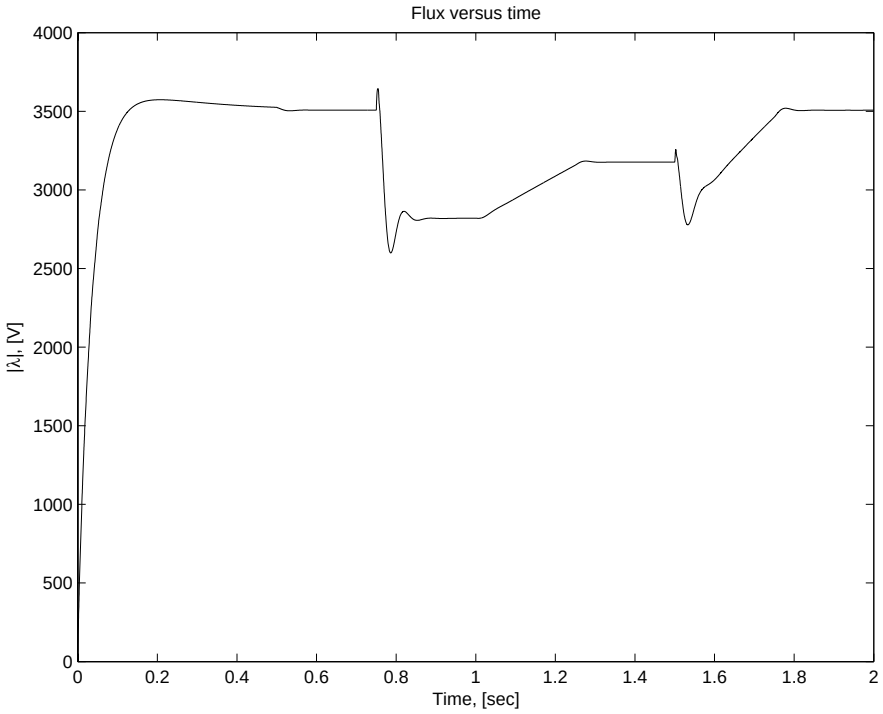


Figure 9.13. Flux response to load changes

### *c. 15 kW Motor Control with Changing Speed*

In order to demonstrate speed control, the motor's speed was adjusted under no-load conditions. Figures 9.14 and 9.15 show the simulation results for the 15-kW motor. The first and second graphs in Figure 9.14 are the commanded speed and actual speed, respectively. The third graph in Figure 9.14 is the motor's phase voltage. Notice that the phase voltage returned to approximately zero when the motor's direction was changed. Figure 9.15 provides the motor's phase current, torque, and flux. The current was uniform except when the motor was changing directions. During direction changes, the current fluctuates around zero just as the voltage did. This was due to the zero crossing of the speed command curve. The torque curve clearly indicates the times of the speed changes. The flux is shown in the third graph of Figure 9.15. It remained constant except during changes in the direction of rotation.

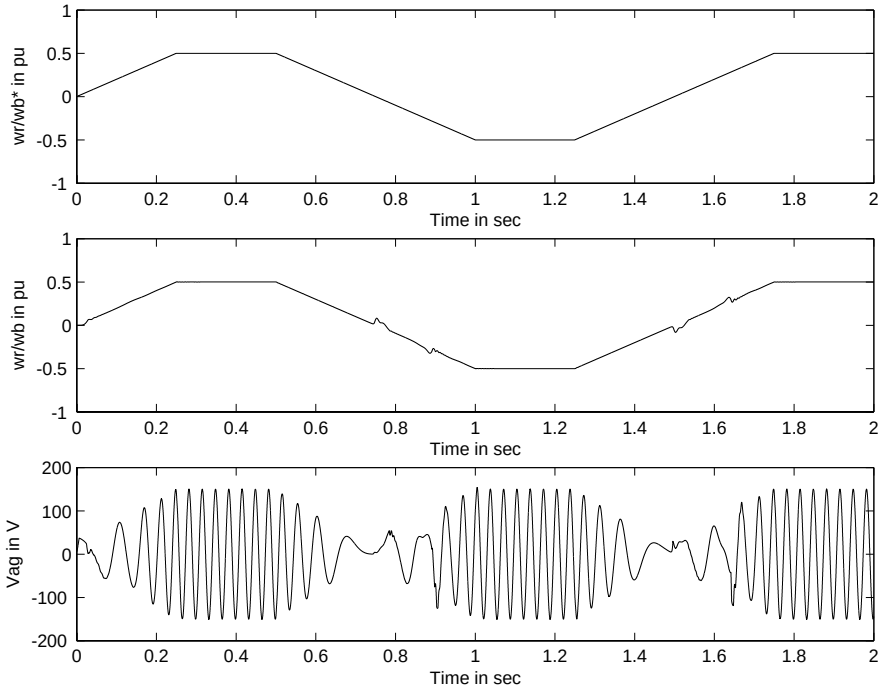


Figure 9.14. 15-kW motor simulation results (From Ref. 32.)

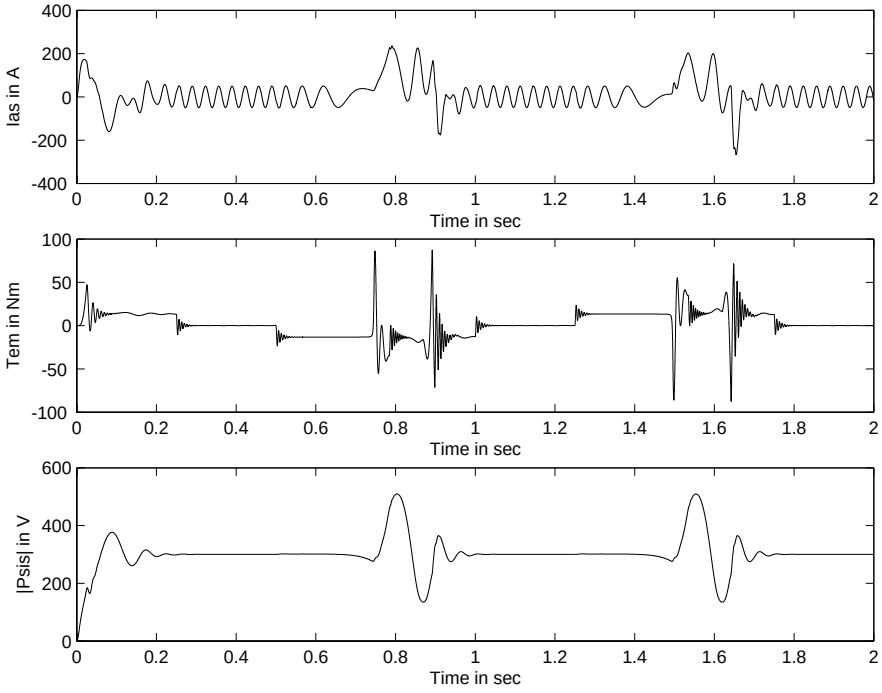


Figure 9.15. 15-kWmotor simulation results (From Ref. 32.)

### *d. 30-MW Motor Control With Changing Speed*

Figures 9-16 through 9-21 provide the results of simulating the 30-MW motor under changing speed conditions. Figure 9-16 is the commanded speed for the motor and figure 9.17 is the rotor's actual speed as the commanded speed is varied. For un-loaded conditions, the rotor speed followed the commanded speed very closely. Figure 9.18 gives the phase voltage response to the speed commands. During the initial change in the direction of rotation, the phase voltage reduced to nearly zero and then returned to the steady state value. When the direction of rotation reversed again, the phase voltage leveled off, but did not become zero. Again, this was due to the motor's large rating. The motor's phase current is shown in figure 9.19. The phase current has the same pattern as the phase voltage. Figure 9.20 shows the torque as the speed was changed. The speed changes are clearly visible on the torque curve. The torque curve for the unloaded motor is much more responsive than the one for the loaded motor. Finally, figure 9.21 shows the change in flux as the speed command was changed. Like the phase current, the flux was relatively uniform with the exception of fluctuations during speed changes.

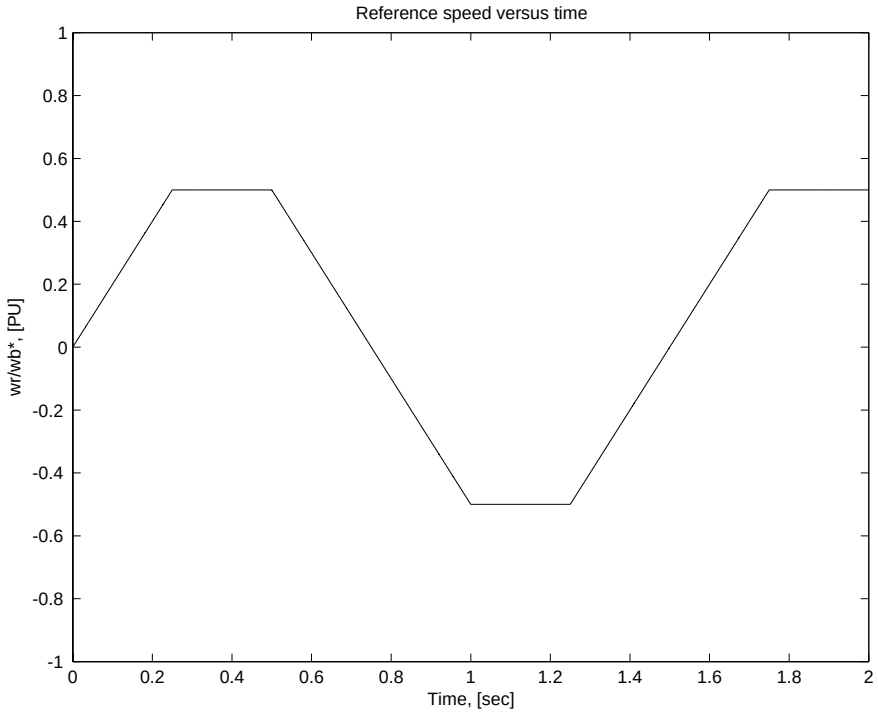


Figure 9.16. Speed command curve

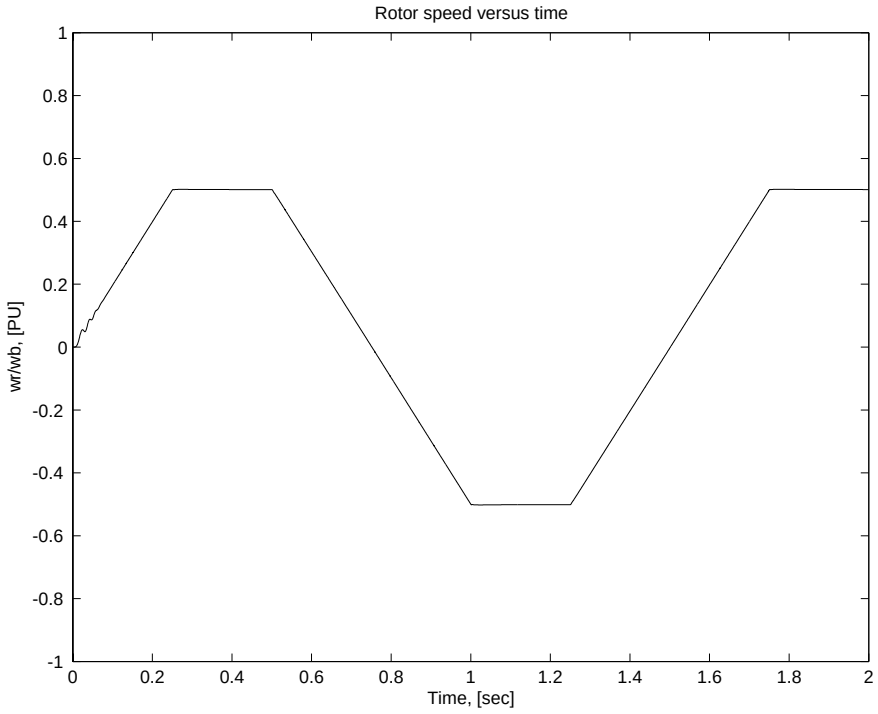


Figure 9.17. Rotor response to changing speed

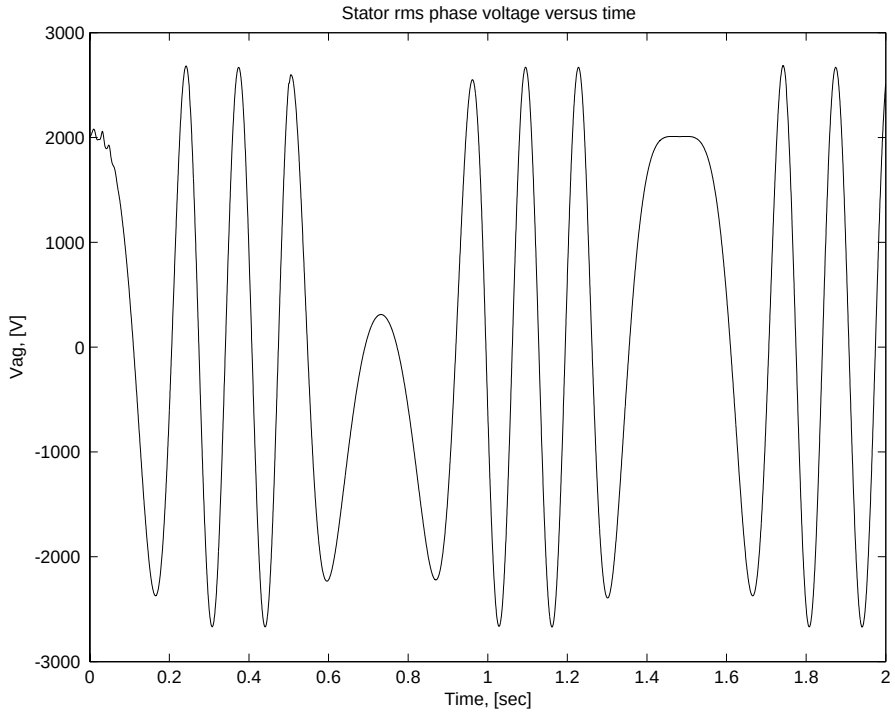


Figure 9.18. Stator RMS phase voltage response to speed changes

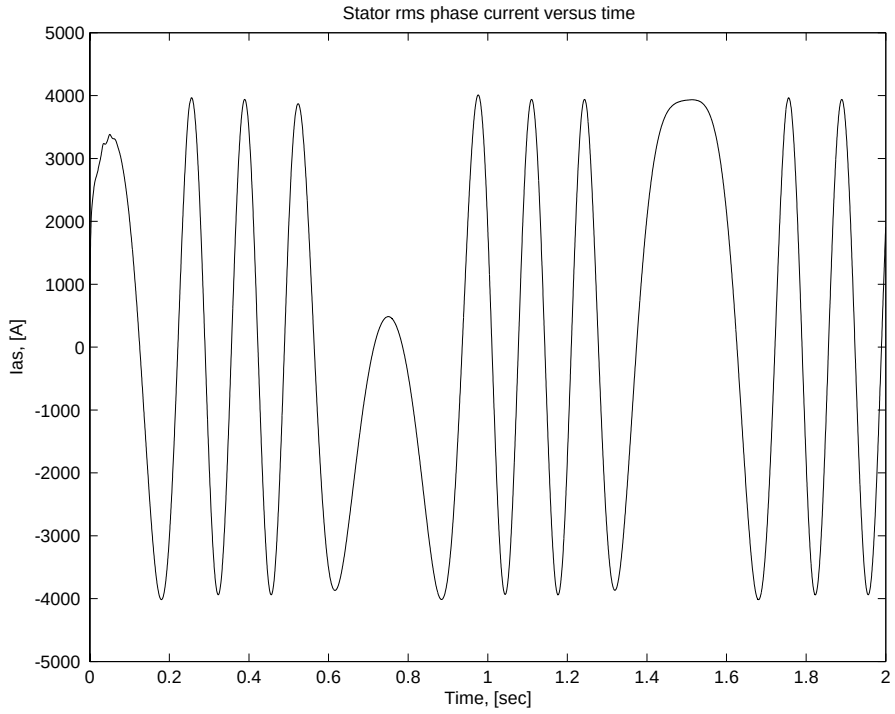


Figure 9.19. Stator RMS phase current response to speed changes

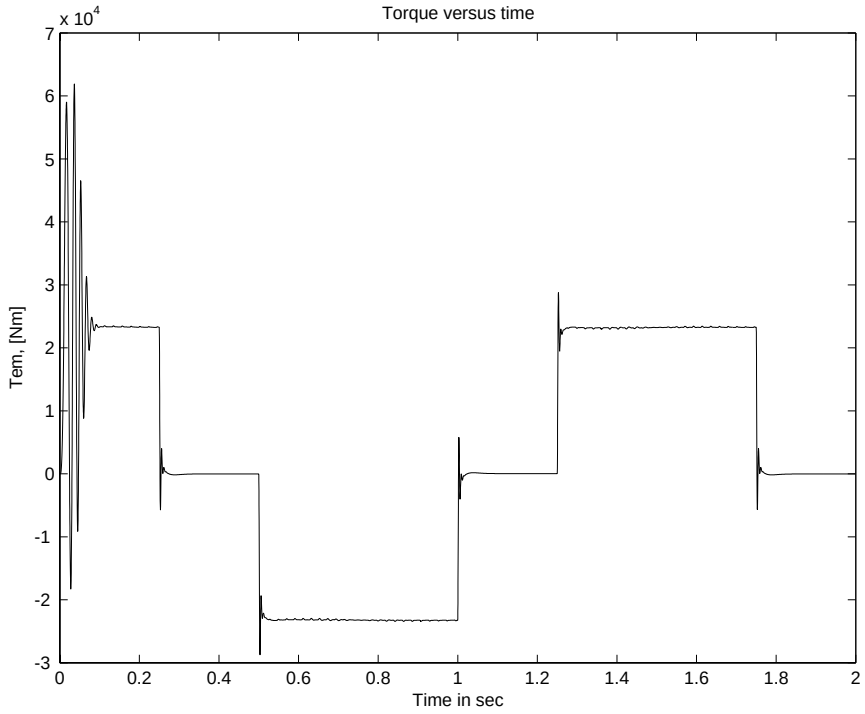


Figure 9.20. Torque response to speed changes

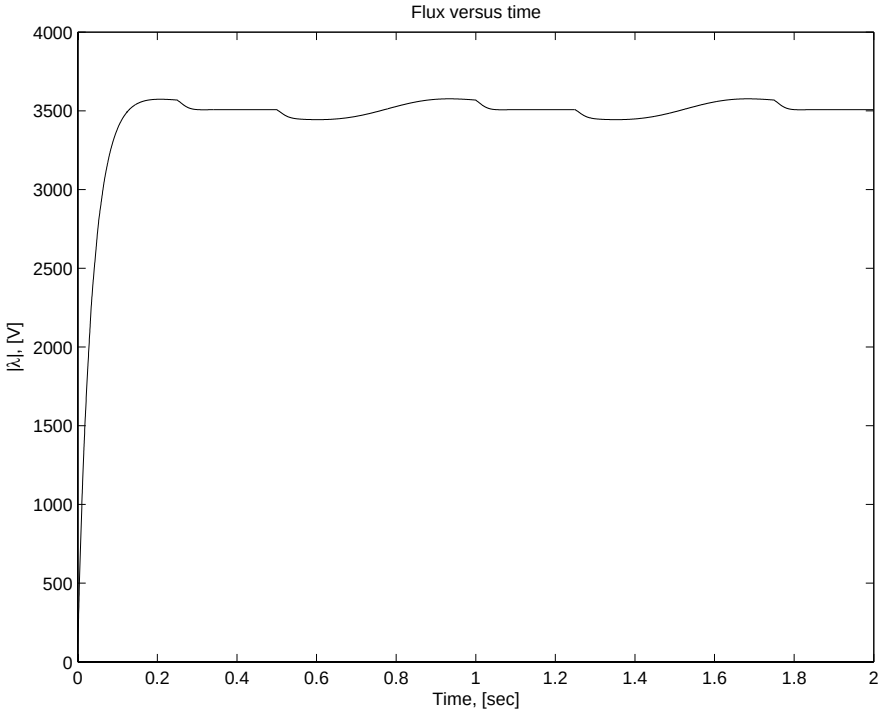


Figure 9.21. Flux response to speed changes

## B. CHAPTER IX CONCLUSION

This chapter has presented the results of a volts/Hertz controlled, 30-MW induction motor simulation and compared them to a 15-kW motor simulation from Reference 32. The simulation was intended to demonstrate the volts/Hertz control method and provide a description of motor operation under changing load and changing speed conditions. Important motor characteristics including phase voltages, currents, speed, flux and torque were plotted and briefly discussed. The simulation results are qualitatively similar to those obtained from the 15-kW machine. There are differences in the simulation results due to the size differences of the two motors. Due to the speed fluctuations and the torque pulsations noticed in the 30-MW simulation, the volts/Hertz control method is not sufficient for large machines requiring precise control. Also, the 30-MW motor is a fictitious motor with variables such as size, power rating, speed of rotation, inductive and resistive components that were chosen to provide a good efficiency and informative simulation results. Less than perfect component selection and other motor parameters also contributed to the differences.

The simulation is relevant to the Navy and to NPS since the Navy will be using electric propulsion in future ships. Further development of the model to include more advanced control methods would benefit anyone desiring to study electric machines.

## C. SUGGESTIONS FOR FUTURE WORK

The Power Program at the Naval Postgraduate School (NPS) provides a good background on the theory of electric machines; however, the control methods that are discussed are limited to stability and frequency response studies. The model and results presented in this chapter provide a foundation for possible future study and further development. Suggestions for future study include the simulation of an induction machine using PWM or PFM control, simulation of a synchronous machine to include an HTS machine, and a simulation involving a DC homopolar machine. Once developed, the models

suggested here could be employed in power classes to demonstrate the properties and control of electric machines.

# X. THESIS CONCLUSION

## A. PURPOSE

The purpose of this thesis was to conduct an evaluation of the electric propulsion options being considered for the U.S. Navy's newest electric ships. Although much of the material in this thesis has been evaluated before, it has not all been included in a single document as it is here. This is a great benefit to anyone desiring to improve their knowledge of the Navy's electric ship program.

## B. THESIS OVERVIEW

Four different motors were examined in this study and they included the induction, synchronous, HTS synchronous, and DC homopolar motor. Each motor has advantages and disadvantages when being considered for ship propulsion. Podded propulsion was briefly reviewed and its potential benefits were discussed. The Navy's IPS program was described and performance-testing results were presented. The test results positively confirmed the IPS concept. The final chapter provided the results of an induction motor simulation under changing load and speed conditions. Simulation results revealed that the volts/Hertz-control method is not sufficient for large motors requiring precise control. More advanced control methods are needed for large motors. The model can be further developed for possible use in NPS power classes. Table 10.1 provides a brief summary of the most important characteristics relating to the motors discussed in this study. As the table indicates, the permanent magnet motor appears to be the best propulsion option when considering fully matured technology. The permanent magnet motor is smaller and weighs less than a comparatively sized induction motor. This supports the Navy's decision to use the permanent magnet motor to provide propulsion in the DD(x). The superconducting motors offer significant volume advantages over the conventional machines. HTS synchronous motor technology is advancing rapidly with the 25 MW motor being produced by AMSC. Progress is being made on the SDCHM, but the unavailability of brush technology is still the largest barrier for this motor.

| | **Induction (AIM-20MW)** | **Permanent Magnet (Jeumont axial flux)** | **HTS Synchronous (25 MW)** | **DC Homopolar (GA Advanced, 19MW)** |
|---|---|---|---|---|
| Efficiency (100% speed) | 97 % | 97 % | 97.5 % | Not Available |
| Weight (tons) | 70 | 65 | 60-70 | 61.2 |
| Volume ($m^3$) | 18.5 | 17.2 | 11.3 | 15 |
| Technology | Mature | Mature | Developing | Developing |

Table 10.1. Comparison of properties for propulsion motors in the 19-25 MW power range.

# APPENDIX A

The induction machine m-file that was used to load the induction machine's parameters for modeling purposes is provided below. The next m-file was used to make speed and load changes during the simulation.

```
% Parameters for 30 MW induction motor

clear all
close all
Sb = 40e3*746;                  % rating in VA
Vrated = 4160;                  % rated line-to-line voltage in V
pf = 0.953;                     % rated power factor
Irated = Sb/(sqrt(3)*Vrated*pf); % rated rms current
P= 12;                          % number of poles
frated = 15;                    % rated frequency in Hz

wb = 2*pi*frated;               % base electrical frequency
we=wb;
wbm = 2*wb/P;                   % base mechanical frequency
Tb = Sb/wbm;                    % base torque
Zb=Vrated*Vrated/Sb;            %base impedance in ohms
Vm = Vrated*sqrt(2/3);          % magnitude of phase voltage
Vb=Vm;
Tfactor = (3*P)/(4*wb);         % factor for torque expression

srated=0.0287; % rated slip
Nrated = 130; % rated speed in rev/min
wmrated=2*pi*Nrated/60; % rated speed in rad/sec
Trated = Sb/wmrated; % rated torque
iasb= 3939; % rated rms phase current

rs = 51e-2;                     % stator wdg resistance in ohms
xls = 6.43e-2;                  % stator leakage reactance in ohms
xplr = xls;                     % rotor leakage reactance in ohms
xm = 82.6e-2;                   % stator magnetizing reactance in ohms
rpr = 52e-2;                    % referred rotor wdg resistance in ohms
xM = 1/(1/xm + 1/xls + 1/xplr);
J = 140e7;      % rotor inertia in kg m2
H = J*wbm*wbm/(2*Sb);           % inertia constant in sec
Domega = 0;                     % rotor damping coefficient

**********************************************************
```

```
% 30 MW induction motor drive using volts/Hertz control (After Ref. 32)

clear all;                          % clear the memory
close all;                          % close all figures
p30mw                               % file for motor parameters
% Calculation of torque speed curves
vas = Vrated/sqrt(3);               % rms phasor voltage
we = wb;                            % excitation frequency
xls = (we/wb)*xls;                  % reactances at excitation frequency
xplr = (we/wb)*xplr;                % reactances at excitation frequency
xm = (we/wb)*xm;                    % reactances at excitation frequency
xM = 1/(1/xm + 1/xls + 1/xplr);
xs = xls + xm;                      % stator self reactance
xr = xplr + xm;                     % rotor self reactance
xsprime = xs - xm*xm/xr;            % stator transient reactance
% Thevenin's equivalent
vth = abs((j*xm/(rs + j*(xls + xm)))*vas);
zth = (j*xm*(rs + j*xls)/(rs + j*(xls + xm )));
rth = real(zth);
xth = imag(zth);
% Compute rotor resistances
rpr1 = sqrt(rth^2 + (xth + xplr)^2);        % rotor resistance for max torque at s=1
% determine smaxt for fixed voltage supply case
smaxt = rpr/rpr1;
%set up vector of rotor resistances
rprv = [rpr];
Nrr=length(rprv);
s = (1:-.02:.02);
N=length(s);
for n=1:N
sn = s(n);
wr(n)=2*we*(1-sn)/P;
for nrr = 1:Nrr
rrn = rprv(nrr);
zin=(rs +j*xls) + j*xm*(rrn/sn + j*xplr)/(rrn/sn + j*(xm + xplr));
ias = vas/zin;
Sin =3*vas*conj(ias);
pin = real(Sin);
pfin(nrr,n)=cos(-angle(ias));
iin(nrr,n)=abs(ias);
te(nrr,n)=(3*P/(2*we))*(vth^2*rrn/sn)/((rth + rrn/sn)^2 + (xth + xplr)^2);
pe(nrr,n)=te(nrr,n)*wr(n);
```

```
eff(nrr,n)=100*pe(nrr,n)/pin;
end % nrr for loop
end % n for loop
% add in synchronous speed values
size(te);
z=[0];
inl=vas/(rs +j*(xls+xm));
inlm = abs(inl);
inla = cos(-angle(inl));
iin=[iin [inlm]'];
pfin=[pfin [inla]'];
eff=[eff z'];
te=[te z'];
pe=[pe z'];
s=[s 0];
wr=[wr 2*we/P];
ns = 120*frated/P;
nr = ns*(1-s);
N=size(wr);
M=size(te);
subplot(2,2,1)
plot(wr,te(1,:),'-')
title('Torque versus Rotor Speed')
xlabel('Rotor Speed, [rad/sec]')
ylabel('Torque, [Nm]')
subplot(2,2,2)
plot(wr,pe(1,:),'-')
title('Power versus Rotor Speed')
xlabel('Rotor speed, [rad/sec]')
ylabel('Power, [W]')
subplot(2,2,3)
plot(wr,iin(1,:),'-')
title('Stator Current versus Rotor Speed')
xlabel('Rotor Speed, [rad/sec]')
ylabel('Stator Current, [A]')
subplot(2,2,4)
plot(wr,eff(1,:),'-')
title('Efficiency versus Rotor Speed')
xlabel('Rotor Speed, [rad/sec]')
ylabel('Efficiency, [%]')
disp('Displaying Operating Characteristics in Fig. 1')
disp(' type " return" to continue');
print -deps -tiff figure(1).eps
keyboard
% determine the volts per hertz table
```

```
%set up vector of excitation frequency
w = (-100:4:100);
emb = j*iasb*xm;
f = w/(2*pi);
N = length(w);
for n = 1:N
we = w(n);
em = abs(we)*emb/wb;
zs = rs + j*(abs(we)/wb)*xls;
vrms(n) = abs(em + iasb*zs);
end
vrms_vf = vrms;
we_vf = w;
clf;
plot(f(:),vrms(:),'-')
title('Stator Phase Voltage versus Frequency')
ylabel('Stator Phase Voltage, [Vrms]')
xlabel('Frequency, [Hz]')
disp('Displaying Volts/Hertz curve, type " return" to continue');
print -deps -tiff figure(2).eps
keyboard
% Transfer to keyboard for simulation
disp('Set for simulation to start from standstill and ')
disp('load cycling at fixed frequency,')
disp('return for plots after simulation by typing " return"');
% setting all initial conditions in SIMULINK simulation to zero
Psiqso = 0;
Psidso = 0;
Psipqro = 0;
Psipdro = 0;
wrbywbo = 0;
% set up speed reference signal for load cycling
time_wref=[0 0.5 4];
speed_wref=[0 1 1]; % speed in per unit
time_tmech=[0 0.75 0.75 1.0 1.25 1.25 1.5 1.5 1.75 2];
tmech_tmech=[0 0 -Trated -Trated -Trated/2 -Trated/2 -Trated/2 -Trated 0 0];
 tstop = 2
keyboard
disp('Plot results in two figure windows')
h1=gcf
figure;
plot(y(:,1),y(:,2),'-')
title('Reference speed versus time')
axis([-inf inf 0 1.2])
xlabel('Time, [sec]')
```

```
ylabel('wr/wb*, [PU]')
print -deps -tiff figure(3).eps
figure;
plot(y(:,1),y(:,5),'-')
title('Rotor speed versus time')
axis([-inf inf 0 1.2])
xlabel('Time, [sec]')
ylabel('wr/wb, [PU]')
print -deps -tiff figure(4).eps
figure;
plot(y(:,1),y(:,3),'-')
title('Stator rms phase voltage versus time')
xlabel('Time, [sec]')
ylabel('Vag, [V]')
print -deps -tiff figure(5).eps
figure;
plot(y(:,1),y(:,6),'-')
title('Stator rms phase current versus time')
xlabel('Time, [sec]')
ylabel('Ias, [A]')
print -deps -tiff figure(6).eps
figure;
plot(y(:,1),y(:,4),'-')
title('Torque versus time')
xlabel('Time, [sec]')
ylabel('Tem, [Nm]')
print -deps -tiff figure(7).eps
figure;
plot(y(:,1),y(:,7),'-')
title('Flux versus time')
xlabel('Time, [sec]')
ylabel('|\lambda|, [V]')
print -deps -tiff figure(8).eps
disp('Save plots in Figs 1 and 2')
disp('Simulation now set for speed cycling at no_load,')
disp('return for plots after simulation by typing " return"');
time_wref=[0 0.25 0.5 1.0 1.25 1.5];
speed_wref=[0 0.5 0.5 -0.5 -0.5 0];
time_tmech=[0 4];
tmech_tmech=[0 0];
keyboard
figure;
plot(y(:,1),y(:,2),'-')
axis([-inf inf -1. 1.])
title('Reference speed versus time')
```

```
xlabel('Time, [sec]')
ylabel('wr/wb*, [PU]')
print -deps -tiff figure(9).eps
figure;
plot(y(:,1),y(:,5),'-')
axis([-inf inf -1. 1.])
title('Rotor speed versus time')
xlabel('Time, [sec]')
ylabel('wr/wb, [PU]')
print -deps -tiff figure(10).eps
figure;
plot(y(:,1),y(:,3),'-')
title('Stator rms phase voltage versus time')
xlabel('Time, [sec]')
ylabel('Vag, [V]')
print -deps -tiff figure(11).eps
figure;
plot(y(:,1),y(:,6),'-')
title('Stator rms phase current versus time')
xlabel('Time, [sec]')
ylabel('Ias, [A]')
print -deps -tiff figure(12).eps
figure;
plot(y(:,1),y(:,4),'-')
title('Torque versus time')
xlabel('Time in sec')
ylabel('Tem, [Nm]')
print -deps -tiff figure(13).eps
figure;
plot(y(:,1),y(:,7),'-')
axis([0 2 0 4000])
title('Flux versus time')
xlabel('Time, [sec]')
ylabel('|\lambda|, [V]')
print -deps -tiff figure(14).eps
disp('Save plots in Figures 1 and 2')
disp('return to exit');
keyboard;

**********************************************************
```

# LIST OF REFERENCES

[1] Edward C. Whitman, "The IPS Advantage. Electric Drive: A Propulsion System for Tomorrow's Submarine Fleet?" *Seapower Magazine*, July 2001.

[2] Robert Ashton, private telephone conversation, April 2003.

[3] J.G. Ciezki and R.W. Ashton, "A Survey of AC Drive Propulsion Options," presented at the 3rd Naval Symposium on Electric Machines, December 4-7, 2000.

[4] J.M. Prousalidis, N.D. Hatziargyriou, and B.C. Papadias, "On Studying Ship Electric Propulsion Motor Driving Schemes" presented at the 4th International Conference on Power System Transients (IPST 2001), Rio de Janeiro, Brazil, June 24-28, 2001.

[5] Chester Petry, "The electric ship and electric weapons", presented at the NDIA 5th System Engineering Conference, Tampa, FL, October 2002, found at http://www.dtic.mil/ndia/2002systems/petry2c3.pdf, last accessed on April 7, 2003.

[6] M. Benatmane, LCDR T. McCoy, T. Dalton, and T.L. Cooper, "Electric power generation and propulsion motor development for U.S. Navy surface ships," *Proceedings All Electric Ship: Developing Benefits for Maritime Appli*cations, The Institute of Marine Engineers, (IMarE) Conference, Vol. 110, (2), pp 53-61, 29-30 September 1998.

[7] Rodney Rempt, "DD-21: Surface Warship for the 21st Century," *Soundoff! Magazine*, August, 2001.

[8] LCDR Timothy McCoy and Makhlouf Benatmane, "The all electric warship: an overview of the U.S. Navy's integrated power system development program," presented at the International Conference on the Electric Ship, September, 1998.

[9] Stephen J. Chapman, *Electric Machinery Fundamentals*, pp. 359-373 and pp. 482-501, McGraw Hill, New York, 1985.

[10] D.M. Kane and M.R. Warburton, "Integration of permanent magnet motor technology," *Power Engineering Society Summer Meeting*, Vol. 1, pp. 275-280, IEEE, 2002.

[11] Raymond Ramshaw and R.G. van Heeswijk, *Energy Conversion: Electric Motors and Generators,* pp. 255-265, Saunders College Publishing, Philadelphia, 1990.

[12] Clive Lewis, "The advanced induction motor," *Power Engineering Society Summer Meeting,* Vol. 1, pp. 250-253, IEEE, 2002.

[13] N. Mohan, T. Underland, W. Robins, *Power Electronics: Converters, Applications and Design*, 2nd edition, pp. 435-438, John Wiley and Sons, New York, 1995.

[14] R. Krishnan, *Electric Motor Drives: Modeling, Analysis, and Control*, Prentice Hall, Upper Saddle River, New Jersey, 2001.

[15] F. Caricchi, F. Crescimbini, and O. Honorati, "Modular axial-flux permanent magnet motor for ship propulsion drives," *IEEE Transactions on Energy Conversion,* Vol. 14, No. 3, pp. 673-676, IEEE, 1999.

[16] M.Rosu, U. Nankuri, A. Arkkio, T. Jokinen, J. Mantere, and J. Westerlund, "Permanent Magnet Synchronous Motor for Ship Propulsion Drives" Helsinki University Laboratory of Electromechanics, unpublished paper.

[17] Yugi Rang, Chenglin Gu, and Huaishu Li, "Analytical design and modeling of a transverse flux PM machine" *Proceedings International Conference on Power System Technology (PowerCon),* Vol. 4, pp. 2164 –2167, 2002.

[18] Kaman Aerospace Corporation, “Kaman Aerospace unit selected to develop propulsion motors for U.S. Navy’s DD(x) destroyer,” press release, August, 2003.

[19] C.G. Hodge and D.J. Mattick, “The electric warship VI,” presented at the meeting of The Institute of Marine Engineers (IMarE), December, 2000.

[20] S. Kalsi, “Development status of superconducting rotating machines,” *Power Engineering Society Winter Meeting*, Vol. 1, pp. 401-403, IEEE, 2002.

[21] David Driscoll, Viatcheslav Dombrovski, Burt Zhang, “Development status of superconducting motors,” *IEEE Power Engineering Review*, Vol. 20 Issue: 5, pp. 12-15, May 2000.

[22] D.I. Driscoll, “A review of superconducting motor technology development,” *Power Engineering Society Winter Meeting*, Vol. 2, pp. 438-441, IEEE, 2001.

[23] Bruce B. Gamble, Swarn Kalsi, Greg Snitchler, David Madura, and Ray Howard, “The status of HTS motors,” *Power Engineering Society Summer Meeting*, Vol. 1, pp. 270 –274, IEEE, 2002.

[24] Michael J. Superczynski, Jr and Donald J. Waltman, ”Homopolar motor with high temperature superconducting field windings,” *IEEE Transactions on Applied Superconductivity*, Vol. 7, No. 2, pp. 513-518, June 1997.

[25] R.J. Thome, W. Creedon, M. Reed, E. Bowles, K. Schaubel, “Homopolar motor technology development,” *Power Engineering Society Summer Meeting*, Vol. 1, pp. 260-264, IEEE, 2002.

[26] “Military applications of superconductivity.” Found at http://members.tripod.com/mikeheiberger/page6.htm. Last accessed on 26 May 2003.

[27] Tom Van Terwisga, Frans Quadvlieg, and Hek Valkhof, "Steerable propulsion units: hydrodynamic issues and design consequences," paper written on the occasion of the 80th anniversary of Schottel GmbH & Co, August 2001, found at http://www.marin.nl/publications/AzimuthingPropulsionUnits_Schottel_2001.pdf. Last accessed March 28, 2003.

[28] Timothy J. McCoy, "Trends in ship electric propulsion," *Power Engineering Society Summer Meeting*, Vol. 1, pp. 343-346, IEEE, 2002.

[29] J.P. Nicod and P. Simon, "A step ahead in electric propulsion with Mermaid," *Proceedings All Electric Ship: Developing Benefits for Maritime Applications*, pp. 217-221, The Institute of Marine Engineers, (IMarE) Conference, Volume 110,2, September, 1998.

[30] Naval Research Advisory Committee, "Infinity Presentation to U.S. Navy," Alstom Corporation, United Kingdom, August 2001.

[31] Thomas Dalton, Ed Harvey, Matt Stauffer, and CDR Chris Mercer, USN, "Final results of the full scale advanced development testing for the integrated power system program," presented at the Association of Scientists and Engineers, 37th Annual Symposium, May, 2000.

[32] Ong, Chee-Mun, *Dynamic Simulation of Electric Machinery using Matlab/Simulink*, pp. 359-373, pp. 426-462, Prentice Hall, Upper Saddle River, New Jersey, 1998.

# INITIAL DISTRIBUTION LIST

1. Defense Technical Information Center
   Ft. Belvoir, VA

2. Dudley Knox Library
   Naval Postgraduate School
   Monterey, CA

3. Robert Ashton, Code Ec/Ah
   Department of Electrical and Computer Engineering
   Naval Postgraduate School
   Monterey, CA

4. Todd Weatherford, Code Ec/Wt
   Department of Electrical and Computer Engineering
   Naval Postgraduate School
   Monterey, CA

5. Chairman, Code Ec
   Department of Electrical and Computer Engineering
   Naval Postgraduate School
   Monterey, CA